

# Intrinsic sign problem in fermionic and bosonic chiral topological matter

Omri Golan,<sup>1,\*</sup> Adam Smith,<sup>2</sup> and Zohar Ringel<sup>3</sup>

<sup>1</sup>*Department of Condensed Matter Physics, Weizmann Institute of Science, Rehovot 76100, Israel*

<sup>2</sup>*Department of Physics, TFK, Technische Universität München,  
James-Frank-Straße 1, D-85748 Garching, Germany*

<sup>3</sup>*Racah Institute of Physics, The Hebrew University of Jerusalem, Jerusalem 9190401, Israel*

The infamous *sign problem* leads to an exponential complexity in Monte Carlo simulations of generic many-body quantum systems. Nevertheless, many phases of matter are known to admit a sign-problem-free representative, allowing efficient simulations on classical computers. Motivated by long standing open problems in many-body physics, as well as fundamental questions in quantum complexity, the possibility of *intrinsic sign problems*, where a phase of matter admits no sign-problem-free representative, was recently raised but remains largely unexplored. Here, we establish the existence of an intrinsic sign problem in a broad class of gapped, chiral, topological phases of matter. Within this class, we exclude the possibility of stoquastic Hamiltonians for bosons (or 'qudits'), and of sign-problem-free determinantal Monte Carlo algorithms for fermions. The intrinsically sign-problematic class of phases we identify is defined in terms of topological invariants with clear observable signatures: the chiral central charge, and the topological spins of anyons. We obtain analogous results for phases that are *spontaneously* chiral, and present evidence for an extension of our results that applies to both chiral and non-chiral topological matter.

## I. INTRODUCTION

Monte Carlo simulations are arguably the most powerful tools for numerically evaluating thermal averages of classical many-body systems, by randomly sampling the phase-space according to the Boltzmann probability distribution [1]. Though the phase-space of an  $N$ -body system scales exponentially with  $N$ , a Monte Carlo approximation with a fixed desired error is usually obtained in polynomial time [2, 3]. In *Quantum* Monte Carlo (QMC), one attempts to perform Monte Carlo computations of thermal averages in quantum many-body systems, by following the heuristic idea that quantum systems in  $d$  dimensions are equivalent to classical systems in  $d + 1$  dimensions [4, 5].

The difficulty with any such quantum to classical mapping, henceforth referred to as a *method*, is the infamous *sign problem*, where the mapping can produce complex, rather than non-negative, Boltzmann weights  $p$ , which do not correspond to a probability distribution. Faced with a sign problem, one can try to change the method used and obtain  $p \geq 0$ , thus *curing the sign problem* [6, 7]. Alternatively, one can perform QMC using the weights  $|p|$ , which is often done but generically leads to an exponential computational complexity in evaluating physical observables, limiting ones ability to simulate large systems at low temperatures [2].

Conceptually, the sign problem can be understood as an obstruction to mapping quantum systems to classical systems, and accordingly, from a number of complexity theoretic perspectives, a generic curing algorithm in polynomial time is not believed to exist [2, 6–10]. In many-body

physics, however, one is mostly interested in universal phenomena, i.e phases of matter and the transitions between them, and therefore representative Hamiltonians which are sign-free often suffice [11]. In fact, QMC simulations continue to produce unparalleled results, in all branches of many-body quantum physics, precisely because new sign-free models are constantly being discovered [5, 11–17].

Designing sign-free models requires *design principles* (or “de-sign” principles) [11, 18] - easily verifiable properties that, if satisfied by a Hamiltonian and method, lead to a sign-free representation of the corresponding partition function. An important example is the condition  $\langle i | H | j \rangle \leq 0$  where  $i \neq j$  label a local basis, which implies non-negative weights  $p$  in a wide range of methods [10, 11]. Hamiltonians satisfying this condition in a given basis are known as *stoquastic* [8], and have proven very useful in both application and theory of QMC in bosonic (or spin, or 'qudit') systems [2, 6–11].

Fermionic Hamiltonians are not expected to be stoquastic in any local basis [2, 5], and alternative methods, collectively known as determinantal quantum Monte-Carlo (DQMC), are therefore used [4, 5, 17, 19, 20]. The search for design principles that apply to DQMC, and applications thereof, has naturally played the dominant role in tackling the sign problem in fermionic systems, and has seen a lot of progress in recent years [5, 17, 18, 21–24]. Nevertheless, long standing open problems in quantum many-body physics continue to defy solution, and remain inaccessible for QMC. These include the nature of high temperature superconductivity and the associated repulsive Hubbard model [20, 25–27], dense nuclear matter and the associated lattice QCD at finite baryon density [28–30], and the enigmatic fractional quantum Hall state at filling  $5/2$  and its associated Coulomb Hamiltonian [31–36], all of which are fermionic.

\* omri.golan@weizmann.ac.il

One may wonder if there is a fundamental reason that no design principle applying to the above open problems has so far been found, despite intense research efforts. More generally,

*Are there phases of matter which do not admit a sign-free representative? Are there physical properties that cannot be exhibited by sign-free models?*

We refer to such phases of matter, where the sign problem simply cannot be cured, as having an *intrinsic sign problem* [9]. From a practical perspective, intrinsic sign problems may prove useful in directing research efforts and computational resources. From a fundamental perspective, intrinsic sign problems identify certain phases of matter as inherently quantum - their physical properties cannot be reproduced by a partition function with positive Boltzmann weights.

To the best of our knowledge, the first intrinsic sign problem was discovered by Hastings [9], who proved that no stoquastic, commuting projector, Hamiltonians exist for the 'doubled semion' phase [37], which is bosonic and topologically ordered. In a parallel work [38], we generalize this result considerably - excluding the possibility of stoquastic Hamiltonians in a broad class of bosonic non-chiral topological phases of matter. Additionally, Reference [39] demonstrated, based on the algebraic structure of edge excitations, that no translationally invariant stoquastic Hamiltonians exist for bosonic chiral topological phases.

In this paper, we establish a new criterion for intrinsic sign problems in chiral topological matter, and take the first step in analyzing intrinsic sign problems in fermionic systems. First, based on the well established 'momentum polarization' method for characterizing chiral topological matter [40–44], we obtain a variant of the result of Ref.[39] - excluding the possibility of stoquastic Hamiltonians in a broad class of bosonic chiral topological phases. We then develop a formalism with which we obtain analogous results for systems comprised of both bosons *and* fermions - excluding the possibility of sign-free DQMC simulations.

All of the above mentioned topological phases are gapped, 2+1 dimensional, and described at low energy by a topological field theory [45–47]. The class of such phases in which we find an intrinsic sign problem is defined in terms of robust data characterizing them: the chiral central charge  $c$ , a rational number, as well as the set  $\{\theta_a\}$  of topological spins of anyons, a subset of roots of unity. Namely, we find that

*An intrinsic sign problem exists if  $e^{2\pi ic/24}$  is not the topological spin of some anyon, i.e.  $e^{2\pi ic/24} \notin \{\theta_a\}$ .*

The above criterion applies to 'most' chiral topological phases, see Table I for examples. In particular, we identify an intrinsic sign problem in 96.7% of the first one-thousand

fermionic Laughlin phases, in all chiral triplet superconductors, and in the three non-abelian candidate phases for the quantum Hall state at filling 5/2. We also find intrinsic sign problems in 91.6% of the first one-thousand  $SU(2)_k$  Chern-Simons theories. Since, for  $k \neq 1, 2, 4$ , these allow for universal quantum computation by manipulation of anyons [48, 49], our results support the strong belief that quantum computation cannot be simulated with classical resources, in polynomial time [50]. This conclusion is strengthened by examining the Fibonacci anyon model, which is known to be universal for quantum computation [49], and is found to be intrinsically sign-problematic.

We stress that both  $c$  and  $\{\theta_a\}$  have clear observable signatures in both the bulk and boundary of chiral topological matter, some of which have been experimentally observed. The chiral central charge controls the boundary thermal Hall conductance [51–54], which was recently measured in quantum Hall and spin systems [31, 55–57]. In the bulk it is predicted to contribute to the Hall (or odd) viscosity at finite wave-vector, as well as in curved background [58–61]. The chiral central charge also affects the angular momentum at conical defects [62], as was recently observed in an optical realization of integer quantum Hall states [63, 64]. The topological spins determine the exchange statistics of anyons, predicted to appear in interferometry experiments [49], though experimental observation remains elusive [65]. A measurement of anyonic statistics via current correlations [66] was recently reported in the Laughlin 1/3 quantum Hall state [67].

The paper is organized as follows. In Sec.II we collect relevant facts regarding chiral topological matter, arriving at the 'momentum polarization' Eq.(3). Section III then obtains Result 1 - an intrinsic sign problem in bosonic chiral topological matter. In Sec.IV we perform a similar analysis for the case where chirality (or time reversal symmetry breaking), appears spontaneously rather than explicitly, arriving at Result 2. We then turn to fermionic systems. In Sec.V we develop a formalism which unifies and generalizes the currently used DQMC algorithms, and the corresponding design principles. In Sec.VI, we obtain within this formalism Result 1F and Result 2F, the fermionic analogs of Results 1 and 2. Section VII describes a conjectured extension of our results that applies beyond chiral phases, and unifies them with the intrinsic sign problems found in our parallel work [38]. In Sec.VIII we discuss our results and provide an outlook for future work.

## II. CHIRAL TOPOLOGICAL MATTER, AND SIGNS FROM GEOMETRIC MANIPULATIONS

In this section we review the necessary details regarding chiral topological phases of matter, and, following Refs.[40–44], obtain the 'momentum polarization' Eq.(3), which is the main tool we use in the remainder of this paper. Later on we will show that gapped bosonic and fermionic Hamil-

TABLE I. Examples of intrinsic sign problems based on the criterion  $e^{2\pi ic/24} \notin \{\theta_a\}$ , in terms of the chiral central charge  $c$  and the topological spins  $\theta_a = e^{2\pi i h_a}$ . The number of spins  $h_a$  is equal to the dimension of the ground state subspace on the torus. We mark bosonic/fermionic phases by (B/F). The quantum Hall Laughlin phases correspond to  $U(1)_q$  Chern-Simons theories. The  $\ell$ -wave superconductor is chiral, e.g  $p + ip$  for  $\ell = 1$ , and spinless. Data for the spinfull case is identical to that of the Chern insulator, with  $-\ell$  odd (even) in place of  $\nu$ , for triplet (singlet) pairing. The modulo 8 ambiguity in the central charge of the Fibonacci anyon model corresponds to the stacking of a given realization with copies of the  $E_8$   $K$ -matrix phase. Data for the three quantum Hall Pfaffian phases is given at the minimal filling  $1/2$ . The physical filling  $5/2$  is obtained by stacking with a  $\nu = 2$  Chern insulator, and an intrinsic sign problem appears in this case as well.

Phase of matter	Parameterization	$c$	$\{h_a\}$	Intrinsic sign problem?
Laughlin (B) [36]	Filling $1/q$ , ( $q \in 2\mathbb{N}$ )	1	$\{a^2/2q\}_{a=0}^{q-1}$	In 98.5% of first $10^3$
Laughlin (F) [36]	Filling $1/q$ , ( $q \in 2\mathbb{N} - 1$ )	1	$\{(a + 1/2)^2/2q\}_{a=0}^{q-1}$	In 96.7% of first $10^3$
Chern insulator (F) [App.B]	Chern number $\nu \in \mathbb{Z}$	$\nu$	$\{\nu/8\}$	For $\nu \notin 12\mathbb{Z}$
$\ell$ -wave superconductor (F) [61]	Pairing channel $\ell \in 2\mathbb{Z} - 1$	$-\ell/2$	$\{-\ell/16\}$	Yes
Kitaev spin liquid (B) [46]	Chern number $\nu \in 2\mathbb{Z} - 1$	$\nu/2$	$\{0, 1/2, \nu/16\}$	Yes
$SU(2)_k$ Chern-Simons (B) [68]	Level $k \in \mathbb{N}$	$3k/(k+2)$	$\{a(a+2)/4(k+2)\}_{a=0}^k$	In 91.6% of first $10^3$
$E_8$ $K$ -matrix (B) [69]	Stack of $n \in \mathbb{N}$ copies	$8n$	$\{0\}$	For $n \notin 3\mathbb{N}$
Fibonacci anyon model (B) [68]		$14/5 \pmod{8}$	$\{0, 2/5\}$	Yes
Pfaffian (F) [70]		$3/2$	$\{0, 1/2, 1/4, 3/4, 1/8, 5/8\}$	Yes
PH-Pfaffian (F) [70]		$1/2$	$\{0, 0, 1/2, 1/2, 1/4, 3/4\}$	Yes
Anti-Pfaffian (F) [70]		$-1/2$	$\{0, 1/2, 1/4, 3/4, 3/8, 7/8\}$	Yes

tonians which are sign-free (due to the an appropriate design principle) cannot obey the aforementioned Eq.(3), unless the chiral central charge and topological spins obey a tight constraint.

### A. Chiral topological matter

A gapped Hamiltonian is said to be in a topological phase of matter if it cannot be deformed to a trivial reference Hamiltonian, without closing the gap. If a symmetry is enforced, only symmetric deformations are considered, and it is additionally required that the symmetry is not spontaneously broken [71, 72]. For Hamiltonians defined on a lattice, as considered in this paper, a natural trivial Hamiltonian is given by the atomic limit of decoupled lattice sites, where the symmetry acts independently on each site.

Topological phases with a unique ground state on the 2-dimensional torus exist only with a prescribed symmetry group, and are termed symmetry protected topological phases (SPTs) [73–75]. When such phases are placed on the cylinder, they support anomalous boundary degrees of freedom which cannot be realized on isolated 1-dimensional spatial manifolds, as well as corresponding quantized bulk response coefficients. Notable examples are the integer quantum Hall states, topological insulators, and topological superconductors [76].

Topological phases with a degenerate ground state subspace on the torus are termed topologically ordered, or symmetry enriched if a symmetry is enforced [77, 78]. Beyond the phenomena exhibited by SPTs, these support localized

quasiparticle excitations with anyonic statistics and fractional charge under the symmetry group. Notable examples are fractional quantum Hall states [49, 79], quantum spin liquids [80], and fractional topological insulators [81, 82].

In this work we consider *chiral* topological phases, where the boundary degrees of freedom that appear on the cylinder propagate unidirectionally. At energies small compared with the bulk gap, the boundary can be described by a chiral conformal field theory (CFT) [83, 84], while the bulk reduces to a chiral topological field theory (TFT) [46, 47], see Fig.1(a). We consider both bosonic and fermionic phases. These may be protected or enriched by an on-site symmetry, but we will not make use of this symmetry in our analysis - only the chirality of the phase will be used.

A notable example for chiral topological phases is given by Chern insulators [85–87]: SPTs protected by the  $U(1)$  fermion number symmetry, which admit free-fermion Hamiltonians. The single particle spectrum of a Chern insulator on the cylinder is depicted in Fig.1(b). Another notable example is the topologically ordered Kitaev spin liquid [46, 88], which can be described by Majorana fermions with a single particle spectrum similar to Fig.1(b), coupled to a  $\mathbb{Z}_2$  gauge field.

Note that the velocity  $v$  of the boundary CFT is a non-universal parameter which generically changes as the microscopic Hamiltonian is deformed. Furthermore, different chiral branches may have different velocities.

The chirality of the boundary CFT and bulk TFT is manifested by their non-vanishing chiral central charge  $c$ , which is rational and *universal* - it is a topological invariant with respect to continuous deformations of the Hamiltonian

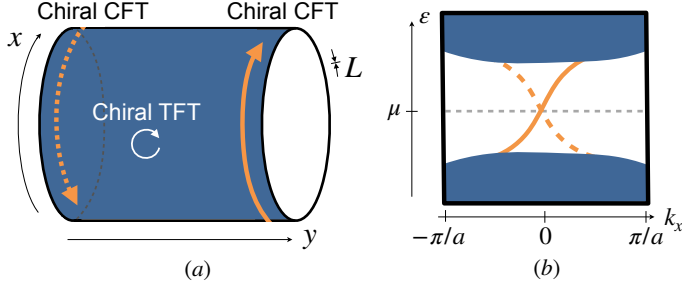


FIG. 1. Chiral topological phases of matter on the cylinder. (a) The low energy description of a chiral topological phase is comprised of two, counter propagating, chiral conformal field theories (CFTs) on the boundary, and a chiral topological field theory (TFT) in the bulk. (b) Examples: schematic single-particle spectrum of a Chern insulator and of the Majorana fermions describing the Kitaev spin liquid. Assuming discrete translational symmetry with spacing  $a$  in the  $x$  direction, one can plot the single-particle eigen-energies  $\epsilon$  on the cylinder as a function of (quasi) momentum  $k_x$ . This reveals an integer number of chiral dispersion branches whose eigen-states are supported on one of the two boundary components. In the Chern insulator (Kitaev spin liquid) these correspond to the Weyl (Majorana-Weyl) fermion CFT, with  $c = \pm 1$  ( $c = \pm 1/2$ ) per branch. The velocity,  $v = |\partial\epsilon/\partial k_x|$  at the chemical potential  $\mu$ , is a non-universal parameter.

which preserve the bulk energy gap, and therefore constant throughout a topological phase [46, 60, 89, 90]. On the boundary  $c$  is defined with respect to an orientation of the cylinder, so the two boundary components have opposite chiral central charges.

### B. Boundary finite size corrections

The non-vanishing of  $c$  implies a number of geometric, or 'gravitational', physical phenomena [58–61, 83, 84, 91, 92]. In particular, the boundary supports a non-vanishing energy current  $J_E$ , which receives a correction

$$J_E(T) = J_E(0) + 2\pi T^2 \frac{c}{24}, \quad (1)$$

at a temperature  $T > 0$ , and in the thermodynamic limit  $L = \infty$ , where  $L$  is the circumference of the cylinder. Note that we set  $K_B = 1$  and  $\hbar = 1$  throughout. Within CFT, this correction is universal since it is independent of  $v$ . Taking the two counter propagating boundary components of the cylinder into account, and placing these at slightly different temperatures, leads to a thermal Hall conductance  $K_H = c\pi T/6$  [51–53], a prediction that recently led to the first measurements of  $c$  [31, 55–57].

In analogy with Eq.(1), the boundary of a chiral topological phase also supports a non-vanishing ground state (at  $T = 0$ ) momentum density  $p$ , which receives a universal

correction on a cylinder with finite circumference  $L < \infty$ ,

$$p(L) = p(\infty) + \frac{2\pi}{L^2} \left( h_0 - \frac{c}{24} \right). \quad (2)$$

Equation (2) is the main property of chiral topological matter that we use below, so we discuss it in detail. First, the rational number  $h_0$  is a *chiral* conformal weight, which is an additional piece of data characterizing the boundary CFT. Like the chiral central charge, the two boundary components of the cylinder have opposite  $h_0$ s. From the bulk TFT perspective,  $h_0$  corresponds to the topological spin of an anyon quasi-particle, defined by the phase  $\theta_0 = e^{2\pi i h_0}$  accumulated as the anyon undergoes a  $2\pi$  rotation [46]. The set  $\{\theta_a\}_{a=1}^N$  of topological spins of anyons is associated with the  $N$ -dimensional ground state subspace on the torus, and the unique  $\theta_0 = e^{2\pi i h_0}$  defined by (2) corresponds to the generically unique ground state on the cylinder, with a finite-size energy separation  $\sim 1/L$  from the low lying excited states, see Appendix A.

As the equation  $\theta_0 = e^{2\pi i h_0}$  suggests, only  $h_0 \bmod 1$  is universal for a topological phase. The integer part of  $h_0$  can change as the Hamiltonian is deformed on the cylinder, while maintaining the bulk gap, and even as a function of  $L$  for a fixed Hamiltonian. Additionally, the choice of  $\theta_0$  from the set  $\{\theta_a\}$  is non-universal, and can change due to bulk gap preserving deformations, or as a function of  $L$ . Both types of discontinuous jumps in  $h_0$  may be accompanied by an accidental degeneracy of the ground state on the cylinder. Therefore, the universal and  $L$ -independent statement regarding  $h_0$  is that, apart from accidental degeneracies,  $e^{2\pi i h_0} = \theta_0 \in \{\theta_a\}$  - a fact that will be important in our analysis.

The non-trivial behavior of  $h_0$  described above appears when the boundary corresponds to a non-conformal deformation of a CFT, by e.g a chemical potential. As demonstrated analytically and numerically in Appendix B, such behavior appears already in the simple context of Chern insulators with non-zero Fermi momenta, as would be the case in Fig.1(b) if the chemical potential  $\mu$  is either raised or lowered.

### C. Momentum polarization

In this section we describe a procedure for the extraction of  $h_0 - c/24$  in Eq.(2), given a lattice Hamiltonian on the cylinder. Since the two boundary components carry opposite momentum densities, the ground state on the cylinder does not carry a total momentum, only a 'momentum polarization'. It is therefore clear that some sort of one-sided translation will be required.

Following Ref.[40], we define  $\tilde{Z} := \text{Tr}(T_R e^{-\beta H})$ , which is related to the usual partition function  $Z = \text{Tr}(e^{-\beta H})$  ( $\beta = 1/T$ ), by the insertion of the operator  $T_R$ , which translates the right half of the cylinder by one unit cell in



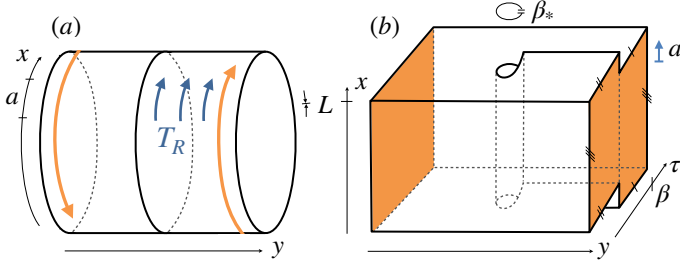


FIG. 2. Momentum polarization. (a) Hamiltonian, or spatial, point of view. The operator  $T_R$  translates the right half of the cylinder by one unit cell, a distance  $a$ , in the  $x$  direction. It acts as the identity on the left boundary component, and as a translation on the right boundary component. The object  $\tilde{Z}/Z$  is the thermal expectation value of  $T_R$ . (b) Field theory, or space-time, point of view. The object  $\tilde{Z}$  is the partition function on a space-time carrying a screw dislocation. The space-time region occupied by the boundary components of the spatial cylinder is colored in orange. The screw dislocation can be described as an additional boundary component, on which  $T_R$  acts as a translation, with a high effective temperature  $1/\beta_*$ .

the periodic  $x$  direction, see Fig.2(a). The object  $\tilde{Z}$  satisfies

$$\tilde{Z} = Z \exp \left[ \alpha N_x + \frac{2\pi i}{N_x} \left( h_0 - \frac{c}{24} \right) + o(N_x^{-1}) \right], \quad (3)$$

where  $N_x$  is the number of sites in the  $x$  direction,  $\alpha \in \mathbb{C}$  is non-universal and has a negative real part, and  $o(N_x^{-1})$  indicates corrections that decay faster than  $N_x^{-1}$  as  $N_x \rightarrow \infty$ . Equation (3) is valid at temperatures low compared to the finite-size energy differences on the boundary,  $\beta^{-1} = o(N_x^{-1})$ , see Appendix A.

Equation (3) follows analytically from the low energy description of chiral topological matter in terms of chiral TFT and CFT [40], and was numerically scrutinized in a large number of examples in Refs.[40–44], as well as in Appendix B. Nevertheless, we are not aware of a rigorous proof of Eq.(3) for gapped lattice Hamiltonians. Therefore, in stating our results we will use the assumption ‘the Hamiltonian  $H$  is in a chiral topological phase of matter’, the content of which is that  $H$  admits a low energy description in terms of a chiral TFT with chiral central charge  $c$  and topological spins  $\{\theta_a\}$ , and in particular, Eq.(3) holds for any bulk-gap preserving deformation of  $H$ , with  $e^{2\pi i h_0} \in \{\theta_a\}$ , apart from accidental degeneracies on the cylinder. In the remainder of this section we further discuss the content of Eq.(3) and its expected range of validity, in light of the Hamiltonian and space-time interpretations of  $\tilde{Z}$ .

From a Hamiltonian perspective,  $\tilde{Z}/Z$  is the thermal expectation value of  $T_R$ , evaluated at a temperature  $\beta^{-1}$  low enough to isolate the ground state. The exponential decay expressed in Eq.(3) appears because  $T_R$  is not a symmetry of  $H$ , and  $-\text{Re}(\alpha)$  can be understood as the energy density of the line defect where  $T_R$  is discontinuous, see Fig.2(a). In fact, we expect Eq.(3) to hold irrespective of whether

the *uniform* translation is a symmetry of  $H$ , or of the underlying ‘lattice’ on which  $H$  is defined, which may be any polygonalization of the cylinder (see Ref.[93] for a similar scenario). The only expected requirement is that the low energy description of  $H$  is homogeneous. Furthermore, if Eq.(3) only holds after a disorder averaging of  $\tilde{Z}/Z$ , our results and derivations in the following sections remain unchanged.

There is also a simple space-time interpretation of  $\tilde{Z}$ , which will be useful in the context of DQMC. The usual partition function  $Z = \text{Tr}(e^{-\beta H})$  has a functional integral representation in terms of bosonic fields  $\phi$  (fermionic fields  $\psi$ ) defined on space, the cylinder  $C$  in our case, and the imaginary time circle  $S^1_\beta = \mathbb{R}/\beta\mathbb{Z}$ , with periodic (anti-periodic) boundary conditions [94]. In  $\tilde{Z} = \text{Tr}(T_R e^{-\beta H})$ , the insertion of  $T_R$  produces a twisting of the boundary conditions of  $\phi, \psi$  in the time direction, such that  $\tilde{Z}$  is the partition function on a space-time carrying a screw dislocation, see Fig.2(b).

The above interpretation of  $\tilde{Z}$ , supplemented by Eq.(2), allows for an intuitive explanation of Eq.(3), which loosely follows its analytic derivation [40]. As seen in Fig.2(b), the line where  $T_R$  is discontinuous can be interpreted as an additional boundary component at a high effective temperature,  $\beta_* \ll L/v$ . Since the effective temperature is much larger than the finite size energy-differences  $2\pi v/L$  on the boundary CFT, the screw dislocation contributes no finite size corrections to  $\tilde{Z}$ . This leaves only the contribution of the boundary component on the right side of the cylinder, where  $T_R$  produces the phase  $e^{iaLp(L)}$ , assuming  $\beta_* \ll L/v \ll \beta$ . Equation (2) then leads to the universal finite size correction  $(2\pi i/N_x)(h_0 - c/24)$ .

### III. EXCLUDING STOQUASTIC HAMILTONIANS FOR CHIRAL TOPOLOGICAL MATTER

In this section we consider bosonic (or ‘qudit’, or spin) systems, and a single design principle - existence of a local basis in which the many-body Hamiltonian is stoquastic. A sketch of the derivation of Result 1 is that the momentum polarization  $\tilde{Z}$  is positive for Hamiltonians  $H'$  which are stoquastic in an on-site and homogenous basis, and this implies that  $\theta_0 = e^{2\pi i c/24}$  for any Hamiltonian  $H$  obtained from  $H'$  by conjugation with a local unitary.

#### A. Setup

The many body Hilbert space is given by  $\mathcal{H} = \otimes_{\mathbf{x} \in X} \mathcal{H}_{\mathbf{x}}$ , where the tensor product runs over the sites  $\mathbf{x} = (x, y)$  of a 2-dimensional lattice  $X$ , and  $\mathcal{H}_{\mathbf{x}}$  are on-site ‘qudit’ Hilbert spaces of finite dimension  $d \in \mathbb{N}$ . With finite-size QMC simulations in mind, we consider a square lattice with spacing 1,  $N_x \times N_y$  sites, and periodic boundary conditions, so that  $X = \mathbb{Z}_{N_x} \times \mathbb{Z}_{N_y}$  is a discretization of the flat torus

$(\mathbb{R}/N_x\mathbb{Z}) \times (\mathbb{R}/N_y\mathbb{Z})$ . Generalization to other 2-dimensional lattices is straight forward. On this Hilbert space a gapped  $r$ -local Hamiltonian  $H = \sum_{\mathbf{x}} H_{\mathbf{x}}$ , which is in a chiral topological phase of matter, is assumed to be given. Here, the terms  $H_{\mathbf{x}}$  are supported within a range  $r$  of  $\mathbf{x}$  - they are defined on  $\otimes_{|\mathbf{y}-\mathbf{x}| \leq r} \mathcal{H}_{\mathbf{y}}$  and act as 0 on all other qudits.

Fix an tensor product basis  $|s\rangle = \otimes_{\mathbf{x} \in X} |s_{\mathbf{x}}\rangle$ , labeled by strings  $s = (s_{\mathbf{x}})_{\mathbf{x} \in X}$ , where  $s_{\mathbf{x}} \in \{1, \dots, d\}$  labels a basis  $|s_{\mathbf{x}}\rangle$  for  $\mathcal{H}_{\mathbf{x}}$ . For any vector  $\mathbf{d} \in X$ , the corresponding translation operator  $T^{\mathbf{d}}$  is defined in this basis,  $T^{\mathbf{d}}|s\rangle = |t^{\mathbf{d}}s\rangle$ , with  $(t^{\mathbf{d}}s)_{\mathbf{x}} = s_{\mathbf{x}+\mathbf{d}}$ . These statements assert that  $|s\rangle$  is both an on-site and a homogeneous basis, or *on-site homogeneous* for short. Note that  $T^{\mathbf{d}}$  acts as a permutation matrix on the  $|s\rangle$ s, and in particular, has non-negative matrix elements in this basis.

In accordance with Sec. II C, we assume that the low energy description of  $H$  is invariant under  $T^{\mathbf{d}}$ , as defined above. In doing so, we exclude the possibility of generic background gauge fields for any on-site symmetry that  $H$  may possess, which is beyond the scope of this work. Nevertheless, commonly used background gauge fields, such as those corresponding to uniform magnetic fields with rational flux per plaquette, can easily be incorporated into our analysis, by restricting to translation vectors  $\mathbf{d}$  in a sub-lattice of  $X$ . A restriction to sub-lattice translations can also be used to guarantee that  $T^{\mathbf{d}}$  acts purely as a translation in the low energy TQFT description. In particular, a lattice translation may permute the anyon types  $a$ <sup>1</sup>. Since the number of anyons is finite, restricting to large enough translations will eliminate this effect. An example is given by Wen's plaquette model, where different anyons are localized on the even/odd sites of a bipartite lattice [95], and a restriction to translations that maps the even (odd) sites to themselves will be made.

Finally, it is assumed that  $H$  is *locally stoquastic*: it is term-wise stoquastic in a local basis. This means that a local unitary operator  $U$  exists, such that the conjugated Hamiltonian  $H' = UH U^\dagger$  is a sum of local terms  $H'_{\mathbf{x}} = UH_{\mathbf{x}}U^\dagger$ , which have non-positive matrix elements in the on-site homogeneous basis,  $\langle s | H'_{\mathbf{x}} | \tilde{s} \rangle \leq 0$  for all basis states  $|s\rangle, |\tilde{s}\rangle$ . Note that we include the diagonal matrix elements in the definition, without loss of generality.

The term *local unitary* used above refers to a depth- $D$  quantum circuit, a product  $U = U_D \cdots U_1$  where each  $U_i$  is itself a product of unitary operators with non-overlapping supports<sup>2</sup> of diameter  $w$ . It follows that  $H'$  has a range  $r' = r + 2r_U$ , where  $r_U = Dw$  is the range of  $U$ . Equivalently, we may take  $U$  to be a finite-time evolution with respect to an  $\tilde{r}$ -local, smoothly time-dependent, Hamiltonian  $\tilde{H}(t)$ , given by the time-ordered exponential  $U = \text{TO} e^{-i \int_0^1 \tilde{H}(t) dt}$ . The two types of locality requirements are equivalent, as

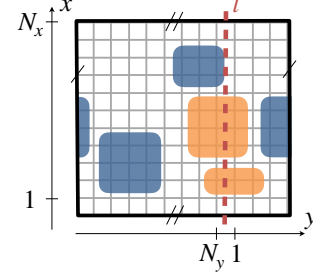


FIG. 3. Cutting the torus to a cylinder along the line  $l$ . Orange areas mark the supports of Hamiltonian terms  $H'_{\mathbf{x}}$  which are removed from  $H'$ , while blue areas mark the supports of terms which are kept.

finite-time evolutions can be efficiently approximated by finite-depth circuits, while finite-depth circuits can be written as finite-time evolutions over time  $D$  with piecewise constant  $w$ -local Hamiltonians [72, 96].

## B. Constraining $c$ and $\{\theta_a\}$

In order to discuss the momentum polarization, we need to map the stoquastic Hamiltonian  $H'$  from the torus  $X$  to a cylinder  $C$ . This is done by choosing a translation vector  $\mathbf{d} \in X$ , and then cutting the torus  $X$  along a line  $l$  parallel to  $\mathbf{d}$ . To simplify the presentation we restrict attention to the case  $\mathbf{d} = (1, 0)$ . All other cases amount to a lattice-spacing redefinition, see Appendix C. The cylinder  $C = \mathbb{Z}_{N_x} \times \{1, \dots, N_y\}$  is then obtained from the torus  $X = \mathbb{Z}_{N_x} \times \mathbb{Z}_{N_y}$  by cutting along the line  $l = \{(i, 1/2) : i \in \mathbb{Z}_{N_x}\}$ . A stoquastic Hamiltonian on the cylinder can be obtained from that on the torus by removing all local terms  $H'_{\mathbf{x}}$  whose support overlaps  $l$ , see Fig. 3. Note that this procedure may render  $H'$  acting as 0 on certain qudits  $\mathcal{H}_{\mathbf{x}}$  with  $\mathbf{x}$  within a range  $r'$  of  $l$ , but this does not bother us. Since all terms  $H'_{\mathbf{x}}$  are individually stoquastic, this procedure leaves  $H'$ , now defined on the cylinder, stoquastic. One can similarly map  $H$  and  $U$  to the cylinder  $C$  such that the relation  $H' = UH U^\dagger$  remains valid on  $C$ .

Let us now make contact with the momentum polarization Eq. (3). Having mapped  $H'$  to the cylinder, we consider the 'partition function'

$$\tilde{Z}' := \text{Tr} \left( e^{-\beta H'} T_R \right), \quad (4)$$

where  $T_R = T_R^{\mathbf{d}}$  is defined by  $T_R |s\rangle = |T_R s\rangle$ ,  $(T_R s)_{x,y} = s_{x+\Theta(y),y}$ , and  $\Theta$  is a heavy side function supported on the right half of the cylinder. Though  $\tilde{Z}'$  is generally different from  $\tilde{Z} = \text{Tr} (e^{-\beta H} T_R)$  appearing in Eq. (3), it satisfies two useful properties:

1.  $\tilde{Z}' > 0$ . Both  $-H'$  and  $T_R$  have non-negative entries in the on-site basis  $|s\rangle$ , and therefore so does  $e^{-\beta H'} T_R$ .

<sup>1</sup> We thank Michael Levin for pointing out this phenomenon.

<sup>2</sup> The support of a unitary  $u = e^{ih}$  is the support of its Hermitian generator  $h$ .

2.  $\tilde{Z}'$  satisfies Eq.(3), with non-universal  $\alpha'$  in place of  $\alpha$ , but  $c' = c$ , and  $h'_0 \in \{\theta_a\}$ . This follows from the fact that  $H' = UHU^\dagger$  is in the same phase of matter as  $H$ , and therefore  $c' = c$ , and  $\{\theta'_a\} = \{\theta_a\}$ . Indeed, treating  $U$  as a finite time evolution, we have  $H(\lambda) = U(\lambda)HU(\lambda)^\dagger$ , where  $U(\lambda) := \text{TO}e^{-i\int_0^\lambda \tilde{H}(t)dt}$ , as a deformation from  $H$  to  $H'$  which maintains locality and preserves the bulk-gap. In fact, since the full spectrum on the cylinder is  $\lambda$ -independent, we have  $h'_0 = h_0$  for all  $N_x$ .

Combining the two above properties leads to

$$1 = \tilde{Z}' / \left| \tilde{Z}' \right| \quad (5)$$

$$= \exp 2\pi i \left[ \epsilon' N_x + \frac{1}{N_x} \left( h_0 - \frac{c}{24} \right) + o(N_x^{-1}) \right],$$

where  $\epsilon' := \text{Im}(\alpha')/2\pi$ . The non-universal integer part of  $h_0$  can then be eliminated by raising Eq.(5) to the  $N_x$ th power,

$$1 = e^{2\pi i \epsilon' N_x^2} \theta_0(N_x) e^{-2\pi i c/24} + o(1), \quad (6)$$

where we used  $\theta_0 = e^{2\pi i h_0}$ , and  $o(1) \rightarrow 0$  as  $N_x \rightarrow \infty$ . We also indicated explicitly the possible  $N_x$ -dependence of  $\theta_0$ , as described in Sec.IIB. We proceed under the assumption that no accidental degeneracies occur on the cylinder, so that  $\theta_0(N_x) \in \{\theta_a\}$  for all  $N_x$ , deferring the degenerate case to Appendix D. Now, for rational  $\epsilon' = n/m$ , the series  $e^{2\pi i \epsilon' N_x^2}$  ( $N_x \in \mathbb{N}$ ) covers periodically a subset  $S$  of the  $m$ th roots of unity, including  $1 \in S$ . On the other hand, for irrational  $\epsilon'$  the series  $e^{2\pi i \epsilon' N_x^2}$  is dense in the unit circle. Combined with the fact that  $\theta_0(N_x)$  is valued in the finite set  $\{\theta_a\}$ , while  $c$  is  $N_x$ -independent, Equation (6) implies that  $\epsilon'$  must be rational, and that the values attained by  $\theta_0(N_x) e^{-2\pi i c/24}$  cover the set  $S$  periodically, for large enough  $N_x$ . It follows that  $1 \in S \subset \{\theta_a e^{-2\pi i c/24}\}$ . We therefore have

**Result 1:** If a local bosonic Hamiltonian  $H$  is both locally stoquastic and in a chiral topological phase of matter, then one of the corresponding topological spins satisfies  $\theta_a = e^{2\pi i c/24}$ . Equivalently, a bosonic chiral topological phase of matter where  $e^{2\pi i c/24}$  is not the topological spin of some anyon, i.e  $e^{2\pi i c/24} \notin \{\theta_a\}$ , admits no local Hamiltonians which are locally stoquastic.

The above result can be stated in terms of the topological  $\mathbf{T}$ -matrix, which is the representation of a Dehn twist on the torus ground state subspace, and has the spectrum  $\text{Spec}(\mathbf{T}) = \{\theta_a e^{-2\pi i c/24}\}_a$  [40, 41, 45, 46, 79, 97].

**Result 1':** If a local bosonic Hamiltonian  $H$  is both locally stoquastic and in a chiral topological phase

of matter, then the corresponding  $\mathbf{T}$ -matrix satisfies  $1 \in \text{Spec}(\mathbf{T})$ . Equivalently, a bosonic chiral topological phase of matter where  $1 \notin \text{Spec}(\mathbf{T})$ , admits no local Hamiltonians which are locally stoquastic.

The above result is our main statement for bosonic phases of matter. The logic used in its derivation will be extended in the following sections, where we generalize Result 1 to systems which are fermionic, spontaneously-chiral, or both.

#### IV. SPONTANEOUS CHIRALITY

The invariants  $h_0$  and  $c$  change sign under both time reversal  $\mathcal{T}$  and parity (spatial reflection)  $\mathcal{P}$ , and therefore require a breaking of  $\mathcal{T}$  and  $\mathcal{P}$  down to  $\mathcal{PT}$  to be non-vanishing. The momentum polarization Eq.(3) is valid if this symmetry breaking is explicit, i.e  $H$  does not commute with  $\mathcal{P}$  and  $\mathcal{T}$  separately. Here we consider the case where  $H$  is  $\mathcal{P}, \mathcal{T}$ -symmetric, but these are broken down to  $\mathcal{PT}$  spontaneously, as in e.g intrinsic topological superfluids and superconductors [61, 98, 99]. We first generalize Eq.(3) to this setting, and then use this generalization to obtain a spontaneously-chiral analog of Result 1.

Note that the physical time-reversal  $\mathcal{T}$  is an *on-site* anti-unitary operator acting *identically* on all qudits, which implies  $[\mathcal{T}, T_R] = 0$ , while  $\mathcal{P}$  is a unitary operator that maps the qudit at  $\mathbf{x}$  to that at  $P\mathbf{x}$ , where  $P$  is the nontrivial element in  $O(2)/SO(2)$ , e.g  $(x, y) \mapsto (-x, y)$ .

##### A. Momentum polarization for spontaneously-chiral Hamiltonians

For simplicity, we begin by assuming that  $H$  is 'classically symmetry breaking' - it has two exact ground states on the cylinder, already at finite system sizes. We therefore have two ground states  $|\pm\rangle$ , such that  $|- \rangle$  is obtained from  $|+ \rangle$  by acting with either  $\mathcal{T}$  or  $\mathcal{P}$ . In particular,  $|\pm\rangle$  have opposite values of  $h_0$  and  $c$ . The  $\beta \rightarrow \infty$  density matrix is then  $e^{-\beta H}/Z = (\rho_+ + \rho_-)/2$ , where  $\rho_\pm = |\pm\rangle\langle\pm|$ , and this modifies the right hand side of Eq.(3) to its real part,

$$\begin{aligned} \tilde{Z} &:= \text{Tr}(T_R e^{-\beta H}) \\ &= Z e^{-\delta N_x} \cos 2\pi \left[ \epsilon N_x + \frac{2\pi}{N_x} \left( h_0 - \frac{c}{24} \right) + o(N_x^{-1}) \right], \end{aligned} \quad (7)$$

where  $-\delta \pm 2\pi i \epsilon$  are the values of the non-universal  $\alpha$  obtained from Eq.(3), by replacing  $e^{-\beta H}$  by  $\rho_\pm$ . Indeed, it follows from  $[\mathcal{T}, T_R] = 0$  that if two density matrices are related by  $\rho_- = \mathcal{T} \rho_+ \mathcal{T}^{-1}$ , then  $\tilde{Z}_\pm := Z_\pm \text{Tr}(T_R \rho_\pm)$  are complex conjugates,  $\tilde{Z}_- = \tilde{Z}_+^*$ .

Now, for a generic symmetry breaking Hamiltonian  $H$ , exact ground state degeneracy happens only in the infinite volume limit [100]. At finite size, the two lowest lying eigenvalues of  $H$  would be separated by an exponentially small energy difference  $\Delta E = O(e^{-f N_x^\lambda})$ , with some

$f > 0, \lambda > 0$ . The two corresponding eigenstates would be  $\mathcal{T}, \mathcal{P}$ -even/odd, of the form  $W[|+\rangle \pm |-\rangle]$ , where  $W$  is a  $\mathcal{T}, \mathcal{P}$ -invariant local unitary [72]. One can think of these statements as resulting from the existence of a bulk-gap preserving and  $\mathcal{T}, \mathcal{P}$ -symmetric deformation of  $H$  to a 'classically symmetry breaking' Hamiltonian<sup>3</sup>.

In the generic setting, we have

$$e^{-\beta H}/Z = W(\rho_+ + \rho_-)W^\dagger/2 + O(\beta\Delta E), \quad (8)$$

and, following our treatment of the local unitary  $U$  in the previous section, Equation (7) remains valid, with modified  $\delta, \epsilon$ , but unchanged  $h_0 - c/24$ . This statement holds for temperatures much higher than  $\Delta E$  and much smaller than the CFT energy spacing,  $\Delta E \ll \beta^{-1} \ll N_x^{-1}$ , or more accurately  $\beta^{-1} = o(N_x^{-1})$  and  $\beta\Delta E = o(N_x^{-1})$  (cf. Sec. II C). Note that the universal content of Eq. (7) is the absolute value  $|h_0 - c/24|$ , since the cosine is even and  $\text{sgn}(\epsilon)$  is non-universal.

### B. Constraining $c$ and $\{\theta_a\}$

Let us now assume that a gapped and local Hamiltonian  $H$  is  $\mathcal{T}, \mathcal{P}$ -symmetric, and is locally stoquastic, due to a unitary  $U$ . It follows that  $\tilde{Z}' = \text{Tr}(T_R e^{-\beta H'}) > 0$ , where  $H' = U H U^\dagger$ . If  $U$  happens to be  $\mathcal{T}, \mathcal{P}$ -symmetric, then so is  $H'$ , and Eq. (7) holds for  $\tilde{Z}'$ , with  $\delta', \epsilon'$  in place of  $\delta, \epsilon$ . For a general  $U$ , we have

$$e^{-\beta H'}/Z' = U W(\rho_+ + \rho_-)W^\dagger U^\dagger/2 + O(\beta\Delta E), \quad (9)$$

where  $UW$  need not be  $\mathcal{T}, \mathcal{P}$ -symmetric. As result,  $\tilde{Z}'$  satisfies a weaker form of Eq. (7),

$$0 < \tilde{Z}' = (Z'/2) \sum_{\sigma=\pm} e^{-\delta'_\sigma N_x} e^{2\pi i \sigma [\epsilon'_\sigma N_x + \frac{1}{N_x}(h_0 - \frac{c}{24}) + o(N_x^{-1})]}, \quad (10)$$

where  $\delta'_+, \epsilon'_+$  may differ from  $\delta'_-, \epsilon'_-$ , and we also indicated the positivity of  $\tilde{Z}'$ . Now, if  $\delta'_+ \neq \delta'_-$ , one of the chiral contributions is exponentially suppressed relative to the other as  $N_x \rightarrow \infty$ , and we can apply the analysis of Sec. III. If  $\delta'_+ = \delta'_-$ , we obtain

$$0 < \sum_{\sigma=\pm} \exp 2\pi i \sigma \left[ \epsilon'_\sigma N_x + \frac{1}{N_x} \left( h_0 - \frac{c}{24} \right) + o(N_x^{-1}) \right], \quad (11)$$

in analogy with Eq. (5). Unlike Eq. (5), taking the  $N_x$ th power of this equation does not eliminate the mod 1 ambiguity in  $h_0$ . This corresponds to the fact that, as opposed to explicitly chiral systems, stacking copies of a spontaneously chiral system does not increase its net chirality. One can replace  $T_R$  in  $\tilde{Z}'$  with a larger half-translation  $T_R^m$ , which would multiply the argument of the cosine by  $m$ . However, since the largest translation on the cylinder is obtained for  $m \approx N_x/2$ , this does not eliminate the mod 1 ambiguity in  $h_0$ . Moreover, even if it so happens that  $\epsilon'_+ = \epsilon'_- = 0$ , Equation (11) does not imply  $h_0 - c/24 = 0 \pmod{1}$  since  $N_x$  is large.

In order to make progress, we make use of the bagpipes construction illustrated in Fig. 4. We attach  $M$  identical cylinders, or 'pipes', to the given lattice, and act with  $T_R$  on these cylinders. The global topology of the given lattice is unimportant - all that is needed is a large enough disk in which the construction can be applied. The construction does require some form of homogeneity in order to have a unique extension of the Hamiltonian  $H'$  to the pipes, and which will be identical for all pipes. We will assume a strict translation symmetry with respect to a sub-lattice, but we believe that this assumption can be relaxed.

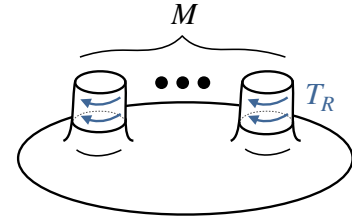


FIG. 4. Bagpipes construction. We attach  $M$  identical cylinders, or 'pipes', to the given lattice, and define the half translation  $T_R$  to act on their top halves, as indicated by blue arrows. The contributions of the pipes to the momentum polarization adds, producing the factor  $M$  in Eq. (12).

The resulting surface, shown in Fig. 4, has negative curvature at the base of each pipe, which requires a finite number of lattice disclinations in this region. In order to avoid any possible ambiguity in the definition of  $H'$  at a disclination, one can simply remove any local term  $H'_x$  whose support contains a disclination, which amounts to puncturing a hole around each disclination. The resulting boundary components do not contribute to the momentum polarization since  $T_R$  acts on these as the identity.

With the construction at hand, the identical contributions of all cylinders to  $\tilde{Z}'$  add, which implies

$$0 < \sum_{\sigma=\pm} \exp 2\pi i \sigma M \left[ \epsilon'_\sigma N_x + \frac{1}{N_x} \left( h_0 - \frac{c}{24} \right) + o(N_x^{-1}) \right]. \quad (12)$$

<sup>3</sup> The canonical example is the transverse field Ising model  $H(g) = -\sum_{i=1}^{N_x} (Z_i Z_{i+1} + g X_i)$  in 1+1d. Exact ground state degeneracy appears at finite  $N_x$  only for  $g = 0$ , though spontaneous symmetry breaking occurs for all  $|g| < 1$ , where a splitting  $\sim |g|^{N_x}$  appears.



Setting  $M = N_x$  gives

$$0 < e^{2\pi i \epsilon'_+ N_x^2} \theta_0(N_x) e^{-2\pi i c/24} + e^{-2\pi i \epsilon'_- N_x^2} \theta_0^*(N_x) e^{2\pi i c/24} + o(1), \quad (13)$$

where we indicate explicitly the possible  $N_x$ -dependence of  $\theta_0$ . This is the spontaneously chiral analog of Eq.(6), and can be analyzed similarly. Since  $\theta_0(N_x)$  is valued in the finite set  $\{\theta_a\}$ , both  $\epsilon'_\pm$  must be rational,  $\epsilon'_\pm = n_\pm/m_\pm$ . Restricting then to  $N_x = n_x m_+ m_-$ , such that  $e^{2\pi i \epsilon_\pm N_x^2} = 1$ , and  $\theta_0$  attains a constant value  $\theta_a$  for large enough  $n_x$ , we have

$$0 < \text{Re}(\theta_a e^{-2\pi i c/24}), \quad (14)$$

for some anyon  $a$ . Repeating the analysis with  $k$  times more pipes  $M = kN_x$ , replaces  $\theta_a e^{-2\pi i c/24}$  in Eq.(14) with its  $k$ th power, for all  $k \in \mathbb{N}$ . This infinite set of equations then implies  $\theta_a e^{-2\pi i c/24} = 1$ . To summarize,

**Result 2:** If a local bosonic Hamiltonian  $H$  is both locally stoquastic and in a spontaneously-chiral topological phase of matter, then one of the corresponding topological spins satisfies  $\theta_a = e^{2\pi i c/24}$ . Equivalently, a bosonic spontaneously-chiral topological phase of matter where  $e^{2\pi i c/24}$  is not the topological spin of some anyon, i.e  $e^{2\pi i c/24} \notin \{\theta_a\}$ , admits no local Hamiltonians which are locally stoquastic.

This extends Result 1 beyond explicitly-chiral Hamiltonians, and clarifies that the essence of the intrinsic sign problem we find is the macroscopic, physically observable, condition  $e^{2\pi i c/24} \notin \{\theta_a\}$ , as opposed to the microscopic absence (or presence) of time reversal and reflection symmetries.

## V. DQMC: LOCALITY, HOMOGENEITY, AND GEOMETRIC MANIPULATIONS

In order to obtain fermionic analogs of the bosonic results of the previous sections, we first need to establish a framework in which such results can be obtained. In this section we develop a formalism that unifies and generalizes the currently used DQMC algorithms and design principles, and implement within it the geometric manipulations used in previous sections, in a sign-free manner. Since we wish to treat the wide range of currently known DQMC algorithms and design principles on equal footing, the discussion will be more abstract than the simple setting of locally stoquastic Hamiltonians used above. In particular, Sections V A-V B lead up to the definition of *locally sign-free DQMC*, which is our fermionic analog of a locally stoquastic Hamiltonian. This definition is used later on in Sec.VI to formulate Result 1F and Result 2F, the fermionic analogs of Results 1 and 2. The new tools needed to establish these results are the sign-free geometric manipulations described in Sec.V D.

### A. Local DQMC

In the presence of bosons and fermions, the many-body Hilbert space is given by  $\mathcal{H} = \mathcal{H}_F \otimes \mathcal{H}_B$ , where  $\mathcal{H}_F$  is a fermionic Fock space, equipped with an on-site occupation basis  $|\nu\rangle_F = \prod_{\mathbf{x},\alpha} (f_{\mathbf{x},\alpha}^\dagger)^{\nu_{\mathbf{x},\alpha}} |0\rangle_F$ ,  $\nu_{\mathbf{x},\alpha} \in \{0,1\}$ , generated by acting with fermionic (anti-commuting) creation operators  $f_{\mathbf{x},\alpha}^\dagger$  on the Fock vacuum  $|0\rangle_F$ . The product is taken with respect to a fixed ordering of fermion species  $\alpha \in \{1, \dots, d_F\}$  and lattice sites  $\mathbf{x} \in X$ . We will also make use of the single-fermion space  $\mathcal{H}_{1F} \cong \mathbb{C}^{|X|} \otimes \mathbb{C}^{d_F}$ , spanned by  $|\mathbf{x}, \alpha\rangle_F = f_{\mathbf{x},\alpha}^\dagger |0\rangle_F$ , where  $|X| = N_x N_y$  is the system size. As in Sec.III,  $\mathcal{H}_B$  is a many-qudit Hilbert space with local dimension  $d$ . It can also be a bosonic Fock space where  $d = \infty$ .

We consider local fermion-boson Hamiltonians  $H$ , of the form

$$H = \sum_{\mathbf{x}, \mathbf{y}} f_{\mathbf{x}}^\dagger h_0^{\mathbf{x}, \mathbf{y}} f_{\mathbf{y}} + H_I, \quad (15)$$

where the free-fermion Hermitian matrix  $h_0^{\mathbf{x}, \mathbf{y}}$  is  $r_0$ -local, it vanishes unless  $|\mathbf{x} - \mathbf{y}| \leq r_0$ , and we suppress, here and in the following, the fermion species indices. The Hamiltonian  $H_I$  describes all possible  $r_0$ -local interactions which preserve the fermion parity  $(-1)^{N_f}$ , where  $N_f = \sum_{\mathbf{x}} f_{\mathbf{x}}^\dagger f_{\mathbf{x}}$ , including fermion-independent terms  $H_B$  as in Sec.III. Thus  $H_I$  is of the form

$$H_I = H_B + \sum_{\mathbf{x}, \mathbf{y}} f_{\mathbf{x}}^\dagger K_B^{\mathbf{x}, \mathbf{y}} f_{\mathbf{y}} + \sum_{\mathbf{x}, \mathbf{y}, \mathbf{z}, \mathbf{w}} f_{\mathbf{x}}^\dagger f_{\mathbf{y}}^\dagger V_B^{\mathbf{x}, \mathbf{y}, \mathbf{z}, \mathbf{w}} f_{\mathbf{z}} f_{\mathbf{w}} + \dots, \quad (16)$$

where  $K_B^{\mathbf{x}, \mathbf{y}}$  (for all  $\mathbf{x}, \mathbf{y} \in X$ ) is a local bosonic operator with range  $r_0$ , and vanishes unless  $|\mathbf{x} - \mathbf{y}| \leq r_0$ , and similarly for  $V_B^{\mathbf{x}, \mathbf{y}, \mathbf{z}, \mathbf{w}}$ , which vanishes unless  $\mathbf{x}, \mathbf{y}, \mathbf{z}, \mathbf{w}$  are contained in a disk or radius  $r_0$ . In Eq.(15) dots represent additional pairing terms of the form  $ff$ ,  $f^\dagger f^\dagger$ , or  $ffff$ ,  $f^\dagger f^\dagger f^\dagger f^\dagger$ , as well as terms with a higher number of fermions, all of which are  $r_0$ -local and preserve the fermion parity.

Since locality is defined in terms of anti-commuting Fermi operators, a local stoquastic basis is not expected to exist, and accordingly, the sign problem appears in any QMC method in which the Boltzmann weights are given in terms of Hamiltonian matrix elements in a local basis [2, 5]. For this reason, the methods used to perform QMC in the presence of fermions are distinct from the ones used in their absence. These are collectively referred to as DQMC [4, 5, 17, 19, 20], and lead to the imaginary time path integral representation of the partition function

$$Z = \text{Tr} (e^{-\beta H}),$$

$$\begin{aligned} Z &= \int D\phi D\psi e^{-S_\phi - S_\psi, \phi} \\ &= \int D\phi e^{-S_\phi} \text{Det} (D_\phi) \\ &= \int D\phi e^{-S_\phi} \text{Det} (I + U_\phi), \end{aligned} \quad (17)$$

involving a bosonic field  $\phi$  with an action  $S_\phi$ , and a fermionic (grassmann valued) field  $\psi$ , with a quadratic action  $S_{\psi, \phi} = \sum_{\mathbf{x}, \mathbf{x}'} \int d\tau \bar{\psi}_{\mathbf{x}, \tau} [D_\phi]_{\mathbf{x}, \mathbf{y}} \psi_{\mathbf{y}, \tau}$  defined by the  $\phi$ -dependent single-fermion operator  $D_\phi$ . In the third line of Eq.(17) we assumed the Hamiltonian form  $D_\phi = \partial_\tau + h_{\phi(\tau)}$ , and used a standard identity for the determinant in terms of the single-fermion imaginary-time evolution operator  $U_\phi = \text{TO} e^{-\int_0^\beta h_{\phi(\tau)} d\tau}$  [19], where TO denotes the time ordering. The field  $\phi$  ( $\psi$ ) is defined on a continuous imaginary-time circle  $\tau \in \mathbb{R}/\beta\mathbb{Z}$ , with periodic (anti-periodic) boundary conditions, and on the spatial lattice  $X$ . The second and third lines of Eq.(17) define the Monte Carlo phase space  $\{\phi\}$  and Boltzmann weight

$$\begin{aligned} p(\phi) &= e^{-S_\phi} \text{Det} (D_\phi) \\ &= e^{-S_\phi} \text{Det} (I + U_\phi). \end{aligned} \quad (18)$$

In applications, the DQMC representation (17) may be obtained from the Hamiltonian  $H$  in a number of ways. If a Yukawa type model is assumed as a starting point [17], i.e  $H_I = H_B + \sum_{\mathbf{x}, \mathbf{y}} f_{\mathbf{x}}^\dagger K_B^{\mathbf{x}, \mathbf{y}} f_{\mathbf{y}}$ , then the action  $S_\phi$  is obtained from the Hamiltonian  $H_B$ , and  $h_{\phi(\tau)} = h_0 + K_B$ . Alternatively, the representation (17) may be obtained through a Hubbard–Stratonovich decoupling and/or a series expansion of fermionic self-interactions [18, 21, 101]. Such is the case e.g when there are no bosons  $\mathcal{H} = \mathcal{H}_F$ , and  $H_I = \sum_{\mathbf{x}, \mathbf{y}} f_{\mathbf{x}}^\dagger f_{\mathbf{y}}^\dagger V^{\mathbf{x}, \mathbf{y}, \mathbf{z}, \mathbf{w}} f_{\mathbf{z}} f_{\mathbf{w}}$ .

To take into account and generalize the above relations between  $H$  and the corresponding DQMC representation, we will only assume (i) that the effective single-fermion Hamiltonian  $h_{\phi(\tau)}$  reduces to the free fermion matrix  $h^{(0)}$  in the absence of  $\phi$ , i.e  $h_{\phi(\tau)=0} = h_0$ , (ii) that the boson field  $\phi$  is itself an  $r_0$ -local object<sup>4</sup>, and (iii) that the  $r_0$ -locality of  $h_0$  and  $H_I$  implies the  $r$ -locality of  $S_\phi$  and  $h_{\phi(\tau)}$ , where  $r$  is some function of  $r_0$ , independent of system size. The physical content of these assumptions is that the fields  $\psi$  and operators  $f$  correspond to the same physical fermion<sup>5</sup>, and that the boson  $\phi$  mediates *all* fermionic interactions

$H_I$ , and therefore corresponds to both the physical bosons in  $\mathcal{H}_B$  and to composite objects made of an even number of fermions within a range  $r_0$  (e.g a Cooper pair  $\phi \sim ff$ ).

We can therefore write

$$\begin{aligned} S_\phi &= \sum_{\tau, \mathbf{x}} S_{\phi; \tau, \mathbf{x}}, \\ h_{\phi(\tau)} &= \sum_{\mathbf{x}} h_{\phi(\tau); \mathbf{x}}, \end{aligned} \quad (19)$$

where each term  $S_{\phi; \tau, \mathbf{x}}$  depends only on the values of  $\phi$  at points  $(\mathbf{x}', \tau')$  with  $|\tau - \tau'|, |\mathbf{x} - \mathbf{x}'| \leq r$ , and similarly, each term  $h_{\phi(\tau); \mathbf{x}}$  is supported on a disk of radius  $r$  around  $\mathbf{x}$ , and depends on the values of  $\phi(\tau)$  at points  $\mathbf{x}$  within this disk.

Note that even though  $H$  is Hermitian, we do not assume the same for  $h_{\phi(\tau)}$ . Non-Hermitian  $h_{\phi(\tau)}$ s naturally arise in Hubbard–Stratonovich decouplings, see e.g [18, 102]. Even when  $h_{\phi(\tau)}$  is Hermitian for all  $\phi$ , its time-dependence implies that  $U_\phi$  is non-Hermitian, and therefore  $\text{Det} (I + U_\phi)$  in Eq.(18) is generically complex valued [19]. This is the generic origin of the sign problem in DQMC. Section VB below describes the notion of *fermionic design principles*, algebraic conditions on  $U_\phi$  implying  $\text{Det} (I + U_\phi) \geq 0$ , and defines what it means for such design principles to be local and homogenous.

In the following analysis, we exclude the case of ‘classically-interacting fermions’, where  $\phi$  is time-independent and  $h_\phi$  is Hermitian. In this case the fermionic weight  $\text{Det} (I + e^{-\beta h_\phi})$  is trivially non-negative, and sign-free DQMC is always possible, provided  $S_\phi \in \mathbb{R}$ . We view such models as ‘exactly solvable’, on equal footing with free-fermion and commuting projector models. Given a phase of matter, the possible existence of exactly solvable models is independent of the possible existence of sign-free models. Even when an exactly solvable model exists, QMC simulations are of interest for generic questions, such as phase transitions due to deformations of the model [103]. In particular, Ref.[104] utilized a classically-free description of Kitaev’s honeycomb model to obtain the thermal Hall conductance and chiral central charge, which should be contrasted with the intrinsic sign problem we find in the corresponding phase of matter, see Table I and Sec.VI.

## B. Local and homogenous fermionic design principles

The representation (17) is sign-free if  $p(\phi) = e^{-S_\phi} \text{Det} (I + U_\phi) \geq 0$  for all  $\phi$ . A design principle then amounts to a set of polynomially verifiable properties<sup>6</sup> of

<sup>4</sup> Thus  $\phi$  is a map from sets of lattice sites with diameter less than  $r_0$ , such as links, plaquettes etc., to a fixed vector space  $\mathbb{C}^k$ . Additionally, the  $\phi$  integration in (17) runs over all such functions. As an example, restricting to constant functions  $\phi$  leads to non-local all to all interactions between fermions.

<sup>5</sup> Technically, via the fermionic coherent state construction of the functional integral [94].

<sup>6</sup> That is, properties which can be verified in a polynomial-in- $\beta|X|$  time. As an example, given a local Hamiltonian, deciding whether there exists a local basis in which it is stoquastic is NP-complete [6, 7]. In particular, one does not need to perform the exponential

$S_\phi$  and  $h_{\phi(\tau)}$  that guarantee that the complex phase of  $\text{Det}(I + U_\phi)$  is opposite to that of  $e^{-S_\phi}$ . For the sake of presentation, we restrict attention to the case where  $S_\phi$  is manifestly real valued, and  $\text{Det}(I + U_\phi) \geq 0$  due to an algebraic condition on the operator  $U_\phi$ , which we write as  $U_\phi \in \mathcal{C}_U$ . This is assumed to follow from an algebraic condition on  $h_{\phi(\tau)}$ , written as  $h_{\phi(\tau)} \in \mathcal{C}_h$ , manifestly satisfied for all  $\phi(\tau)$ . The set  $\mathcal{C}_h$  is assumed to be closed under addition, while  $\mathcal{C}_U$  is closed under multiplication:  $h_1 + h_2 \in \mathcal{C}_h$  for all  $h_1, h_2 \in \mathcal{C}_h$ , and  $U_1 U_2 \in \mathcal{C}_U$  for all  $U_1, U_2 \in \mathcal{C}_U$ .

The simplest example, where  $\mathcal{C}_U = \mathcal{C}_h$  is the set of matrices obeying a fixed time reversal symmetry, is discussed in Sec. V C. In Appendix F we review all other design principles known to us, demonstrate that most of them are of the simplified form above, and generalize our arguments to those that are not. Comparing with the bosonic Hamiltonians treated in Sec. III, we note that  $\mathcal{C}_h$  is analogous to the set of stoquastic Hamiltonians  $H$  in a fixed basis, while  $\mathcal{C}_U$  is analogous to the resulting set of matrices  $e^{-\beta H}$  with non-negative entries.

Design principles, as defined above (and in the literature), are purely algebraic conditions, which carry no information about the underlying geometry of space-time. However, as demonstrated in Sec. V C, in order to allow for local interactions, mediated by an  $r_0$ -local boson  $\phi$ , a design principle must also be local in some sense. We will adopt the following definitions, which are shown to be satisfied by all physical applications of design principles that we are aware of, in Sec. V C and Appendix F.

*Definition (term-wise sign-free):* We say that a DQMC representation is term-wise sign-free due to a design principle  $\mathcal{C}_h$ , if each of the local terms  $S_{\phi;\tau,\mathbf{x}}, h_{\phi(\tau);\mathbf{x}}$  obey the design principle separately, rather than just their sums  $S_\phi, h_{\phi(\tau)}$ . Thus  $S_{\phi;\tau,\mathbf{x}}$  is real valued, and  $h_{\phi(\tau);\mathbf{x}} \in \mathcal{C}_h$ , for all  $\tau, \mathbf{x}$ .

This is analogous to the requirement in Sec. III A that  $H'$  be term-wise stoquastic. Note that even when a DQMC representation is term-wise sign-free, the resulting Boltzmann weights  $p(\phi)$  are sign-free in a non-local manner:  $\text{Det}(I + U_\phi)$  involves the values of  $\phi$  at all space-time points, and splitting the determinant into a product of local terms by the Leibniz formula reintroduces signs, which capture the fermionic statistics. In this respect, the ‘‘classical’’ Boltzmann weights  $p(\phi)$  are always non-local in DQMC.

*Definition (on-site homogeneous design principle):* A design principle is said to be on-site homogenous if any permutation of the lattice sites  $\sigma \in S_X$  obeys it. That is, the operator

$$O_{(\mathbf{x},\alpha),(\mathbf{x}',\alpha')}^{(\sigma)} = \delta_{\mathbf{x},\sigma(\mathbf{x}')}\delta_{\alpha,\alpha'}, \quad (20)$$

---

operation of evaluating  $p$  on every configuration  $\phi$  to assure that  $p(\phi) \geq 0$ . Had this been possible, there would be no need for a Monte Carlo sampling of the phase space  $\{\phi\}$ .

viewed as a single-fermion imaginary-time evolution operator, obeys the design principle,  $O^{(\sigma)} \in \mathcal{C}_U$ , for all  $\sigma \in S_X$ .

This amounts to the statement that the design principle treats all lattice sites on equal footing, since it follows that  $U_\phi \in \mathcal{C}_U \Rightarrow O^{(\sigma)} U_\phi O^{(\bar{\sigma})} \in \mathcal{C}_U$  for all permutations  $\sigma, \bar{\sigma}$ . It may be that a design principle is on-site only with respect to a sub-lattice  $X' \subset X$ . In this case we simply treat  $X'$  as the spatial lattice, and add the finite set  $X/X'$  to the  $\mathbf{d}_F$  internal degrees of freedom. Comparing with Sec. III A, on-site homogenous design principles are analogous to the set of Hamiltonians  $H'$  which are stoquastic in an on-site homogenous basis - any qudit permutation operator has non-negative entries in this basis, like the imaginary time evolution  $e^{-\beta H'}$ .

With these two notions of locality and homogeneity in design principles, we now define the DQMC analog of locally stoquastic Hamiltonians (see Sec. III).

*Definition (locally sign-free DQMC):* Given a local fermion-boson Hamiltonian  $H$ , we say that  $H$  allows for a locally sign-free DQMC simulation, if there exists a local unitary  $U$ , such that  $H' = U H U^\dagger$  has a local DQMC representation (17), which is term-wise sign-free due to an on-site homogeneous design principle.

Note that the DQMC representation (17) is not of the Hamiltonian but of the partition function, and clearly  $Z' = \text{Tr}(e^{-\beta H'}) = \text{Tr}(e^{-\beta H}) = Z$ . What the above definition entails, is that it is  $H'$ , rather than  $H$ , from which the DQMC data  $S_\phi, h_{\phi(\tau)}$  is obtained, as described in Sec. V A. This data is then assumed to be term-wise sign-free due to an on-site homogeneous design principle. The local unitary  $U$  appearing in the above definition is generally fermionic [105]: it can be written as a finite time evolution  $U = \text{TO} e^{-i \int_0^1 \tilde{H}(t) dt}$ , where  $\tilde{H}$  is a local fermion-boson Hamiltonian, which is either piecewise-constant or smooth as a function of  $t$ , c.f. Sec. III A.

### C. Example: time reversal design principle

To demonstrate the above definitions in a concrete setting, consider the time-reversal design principle, defined by an anti-unitary operator  $\mathbb{T}$  acting on the single-fermion Hilbert space  $\mathcal{H}_{1F} \cong \mathbb{C}^{|X|} \otimes \mathbb{C}^{\mathbf{d}_F}$ , such that  $\mathbb{T}^2 = -I$ . The set  $\mathcal{C}_h$  contains all  $\mathbb{T}$ -invariant matrices,  $[\mathbb{T}, h_{\phi(\tau)}] = 0$ . It follows that  $[\mathbb{T}, U_\phi] = 0$ , so that  $\mathcal{C}_U = \mathcal{C}_h$  in this case, and this implies  $\text{Det}(I + U_\phi) \geq 0$  [28, 102].

A sufficient condition on  $\mathbb{T}$  that guarantees that the design principle it defines is on-site homogenous is that it is of the form  $\mathbb{T}_0 = I_{|X|} \otimes \mathbf{t}$ , where  $I_{|X|}$  is the identity matrix on  $\mathbb{C}^{|X|}$ , and  $\mathbf{t}$  is an anti-unitary on  $\mathbb{C}^{\mathbf{d}_F}$  that squares to  $-I_{\mathbf{d}_F}$ . Equivalently,  $\mathbb{T}$  is block diagonal, with identical blocks  $\mathbf{t}$  corresponding to the lattice sites  $\mathbf{x} \in X$ . It is then clear that the permutation matrices  $O^{(\sigma)}$  defined

in Eq.(20) commute with  $\mathsf{T}$ , so  $O^{(\sigma)} \in \mathcal{C}_U$  for all  $\sigma \in S_X$ . Note that the design principle  $\mathsf{T}$  may correspond to a *physical* time-reversal  $\mathcal{T}$ , discussed in Sec.IV, only if it is on-site homogenous, which is why we distinguish the two in our notation.

Additionally, if the operator  $\mathsf{T}$  is  $r_{\mathsf{T}}$ -local with some range  $r_{\mathsf{T}} \geq 0$ , then any local  $h_{\phi(\tau)}$  which is sign-free due to  $\mathsf{T}$  can be made term-wise sign-free. Indeed, if  $[\mathsf{T}, h_{\phi(\tau)}] = 0$  then

$$\begin{aligned} h_{\phi(\tau)} &= \frac{1}{2} (h_{\phi(\tau)} + \mathsf{T} h_{\phi(\tau)} \mathsf{T}^{-1}) \\ &= \sum_{\mathbf{x}} \frac{1}{2} (h_{\phi(\tau); \mathbf{x}} + \mathsf{T} h_{\phi(\tau); \mathbf{x}} \mathsf{T}^{-1}) \\ &= \sum_{\mathbf{x}} \tilde{h}_{\phi(\tau); \mathbf{x}}, \end{aligned} \quad (21)$$

where  $\tilde{h}_{\phi(\tau); \mathbf{x}}$  is now supported on a disk of radius  $r + 2r_{\mathsf{T}}$  and commutes with  $\mathsf{T}$ , for all  $\mathbf{x}$ . We see that the specific notion of  $r_{\mathsf{T}}$ -locality coincides with the general notion of 'term-wise sign free'. In particular,  $\mathsf{T} = \mathsf{T}_0$  has a range  $r_{\mathsf{T}} = 0$ , and can therefore be applied term-wise.

The above statements imply that if  $\mathsf{T} = u \mathsf{T}_0 u^\dagger$ , where  $u$  is a single-fermion local unitary, and  $H$  has a local DQMC representation which is sign-free due to  $\mathsf{T}$ , then  $H$  allows for a locally sign-free DQMC simulation. Indeed, extending  $u$  to a many-body local unitary  $U$ , we see that  $H' = U H U^\dagger$  admits a local DQMC representation where  $[\mathsf{T}_0, h'_{\phi(\tau)}] = 0$ . Since  $\mathsf{T}_0$  is on-site homogenous, and  $h'_{\phi(\tau)}$  can be assumed term-wise sign-free (see Eq.(21)), we have the desired result. As demonstrated in Appendix F, much of the above analysis carries over to other known design principles.

All realizations of  $\mathsf{T}$  presented in Ref.[102] in the context of generalized Hubbard models, and in Ref.[17] in the context of quantum critical metals, have the on-site homogeneous form  $\mathsf{T}_0$ , and therefore correspond to locally sign-free DQMC simulations.

We now consider a few specific time-reversal design principles  $\mathsf{T}$ . The physical spin-1/2 time reversal  $\mathsf{T} = \mathcal{T}^{(1/2)}$ , where  $\mathcal{T}_{(\mathbf{x}, \alpha), (\mathbf{x}', \alpha')}^{(1/2)} = \delta_{\mathbf{x}, \mathbf{x}'} \varepsilon_{\alpha \alpha'} \mathcal{K}$ , and  $\alpha, \alpha' \in \{\uparrow, \downarrow\}$  correspond to up and down spin components, is an on-site homogeneous design principle, which accounts for the absence of signs in the attractive Hubbard model [102]. The composition  $\mathsf{T} = \mathcal{M} \mathcal{T}^{(1/2)}$  of  $\mathcal{T}^{(1/2)}$  with a modulo 2 translation,  $\mathcal{M}_{(\mathbf{x}, \alpha), (\mathbf{x}', \alpha')} = \delta_{(-1)^x, (-1)^{x'+1}} \delta_{x_e, x'_e} \delta_{y, y'} \delta_{\alpha, \alpha'}$ , where  $x_e = 2 \lfloor x/2 \rfloor$  is the even part of  $x$ , is an on-site homogeneous design principle with respect to the sub-lattice  $X' = \{(2x_1, x_2) : \mathbf{x} \in X\}$ , but not with respect to  $X$ . On the other hand, the composition  $\mathsf{T} = \mathcal{P}^{(0)} \mathcal{T}^{(1/2)}$  of  $\mathcal{T}^{(1/2)}$  with a spin-less reflection (or parity)  $\mathcal{P}_{(\mathbf{x}, \alpha), (\mathbf{x}', \alpha')}^{(0)} = \delta_{x, -x'} \delta_{y, y'} \delta_{\alpha \alpha'}$ , is not on-site homogeneous with respect to any sub-lattice.

The latter example is clearly non-local, and we use it to demonstrate the necessity of locality in design principles.

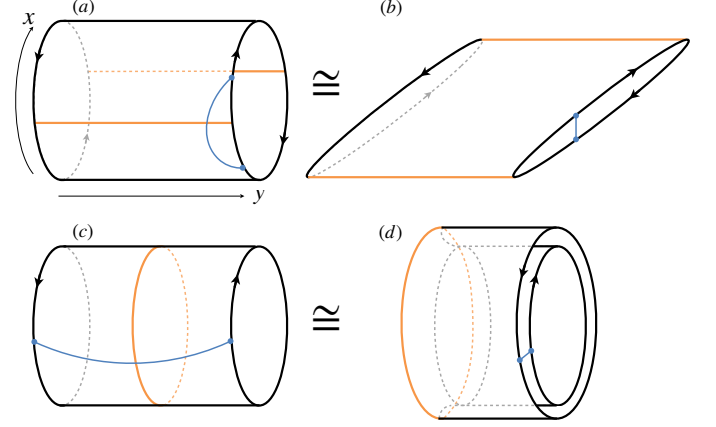


FIG. 5.  $\mathcal{PT}$  symmetry as a 'non-local design principle' for chiral topological matter. (a), (c):  $\mathcal{PT}$  symmetry, where  $\mathcal{P}$  is a reflection (with respect to the orange lines) and  $\mathcal{T}$  is an on-site time-reversal, is a natural symmetry in chiral topological phases. If  $(\mathcal{PT})^2 = -I$ , as is the case when  $\mathcal{P} = \mathcal{P}^{(0)}$  is spin-less and  $\mathcal{T} = \mathcal{T}^{(1/2)}$  is spin-full, it implies the non-negativity of fermionic determinants. Nevertheless, as  $\mathcal{PT}$  is non-local, it only allows for QMC simulations with  $\mathcal{PT}$  invariant bosonic fields, which mediate non-local interactions (blue lines) between fermions. Arrows indicate the chirality of boundary degrees of freedom. (b), (d): Such non-local interactions effectively fold the system into a non-chiral locally-interacting system supported on half the cylinder, where  $\mathcal{PT}$  acts as an on-site time reversal. In particular, the boundary degrees of freedom are now non-chiral. Thus,  $\mathcal{PT}$  does not allow for sign-free QMC simulations of chiral topological matter. More generally, fermionic design principles must be local in order to allow for sign-free DQMC simulations of local Hamiltonians.

As discussed in Sec.IV, the breaking of  $\mathcal{P}$  and  $\mathcal{T}$  down to  $\mathcal{PT}$  actually defines the notion of chirality, and therefore  $\mathcal{PT}$  is a natural symmetry in chiral topological matter. Accordingly, the design principle  $\mathsf{T} = \mathcal{P}^{(0)} \mathcal{T}^{(1/2)}$  applies to a class of models for chiral topological phases, see Appendix E. This seems to allow, from the naive algebraic perspective, for a sign-free DQMC simulation of certain chiral topological phases. However, the weights  $p(\phi)$  will only be non-negative for bosonic configurations  $\phi$  which are invariant under  $\mathsf{T} = \mathcal{P}^{(0)} \mathcal{T}^{(1/2)}$ . Restricting the  $\phi$  integration in Eq.(17) to such configurations leads to non-local interactions between fermions  $\psi$ , coupling the points  $(x, y)$  and  $(-x, y)$ . These interactions effectively fold the non-local chiral system into a local non-chiral system of half of space, see Fig.5. Thus,  $\mathsf{T} = \mathcal{P}^{(0)} \mathcal{T}^{(1/2)}$  does *not* allow for sign-free DQMC simulations of chiral topological matter.

#### D. Sign-free geometric manipulations in DQMC

Let  $Z$  be a partition function in a local DQMC form (17), on the discrete torus  $X = \mathbb{Z}_{N_x} \times \mathbb{Z}_{N_y}$  and imaginary time circle  $S^1_\beta = \mathbb{R}/\beta\mathbb{Z}$ , which is term-wise sign-free



due to an on-site homogenous design principle. In this section we show that it is possible to cut  $X$  to the cylinder  $C$ , and subsequently introduce a screw dislocation in the space-time  $C \times S_\beta^1$ , which corresponds to the momentum polarization (3), while maintaining the DQMC weights  $p(\phi)$  non-negative.

### 1. Introducing spatial boundaries

Given a translation  $T^{\mathbf{d}}$  ( $\mathbf{d} \in X$ ), we can cut the torus  $X$  along a line  $l$  parallel to  $\mathbf{d}$ , and obtain a cylinder  $C$  where  $T^{\mathbf{d}}$  acts as a translation within each boundary component, as in Sec.III. Given the QMC representation (17), the corresponding representation on  $C$  is obtained by eliminating all local terms  $S_{\phi;\tau,\mathbf{x}}, h_{\phi(\tau);\mathbf{x}}$  whose support overlaps  $l$ , as in Fig.3. This procedure may render  $S_\phi, h_{\phi(\tau)}$  independent of certain degrees of freedom  $\phi(\mathbf{x}, \tau), \psi(\mathbf{x}, \tau)$ , with  $\mathbf{x}$  within a range  $r$  of  $l$ , in which case we simply remove such degrees of freedom from the functional integral (17)<sup>7</sup>. Since  $S_{\phi;\tau,\mathbf{x}}, h_{\phi(\tau);\mathbf{x}}$  obey the design principle for every  $\mathbf{x}, \tau$ , the resulting  $S_\phi, h_{\phi(\tau)}$  still obey the design principle and the weights  $p(\phi)$  remain real and non-negative.

### 2. Introducing a screw dislocation in space-time

Let us now restrict attention to  $\mathbf{d} = (1, 0)$ , and make contact with the momentum polarization (3). Given a partition function on the space-time  $C \times S_\beta^1$ , consider twisting the boundary conditions in the time direction,

$$\begin{aligned}\phi_{\tau+\beta, x, y} &= \phi_{\tau, x-\lambda\Theta(y), y}, \\ \psi_{\tau+\beta, x, y} &= -\psi_{\tau, x-\lambda\Theta(y), y}.\end{aligned}\quad (22)$$

Note that  $\lambda \in \mathbb{Z}_{N_x}$ , since  $x \in \mathbb{Z}_{N_x}$ . In particular, the full twist  $\lambda = N_x$  is equivalent to the untwisted case  $\lambda = 0$ , which is equivalent to the statement that the modular parameter of the torus is defined mod 1 (see e.g example 8.2 of [106]). The case  $\lambda = 0$  gives the standard boundary conditions, where the partition function is, in Hamiltonian terms, just  $Z = \text{Tr}(e^{-\beta H})$ . In this case  $Z > 0$  since  $H$  is Hermitian, though its QMC representation  $Z = \sum_\phi p(\phi)$  will generically involve complex valued weights  $p$ . The twisted case  $\lambda = 1$  includes the insertion of the half-translation operator

$$\tilde{Z} = \text{Tr}(T_R e^{-\beta H}), \quad (23)$$

which appears in the momentum polarization (3). Since  $T_R$  is unitary rather than hermitian,  $\tilde{Z}$  itself will generically be complex. However,

*Claim:* If  $Z$  has a DQMC representation (17), with  $p(\phi) \geq 0$  term-wise due to an on-site homogeneous design principle  $\mathcal{C}_U$ , then  $\tilde{Z}$  has a QMC representation  $\tilde{Z} = \sum_\phi \tilde{p}(\phi)$ , with  $\tilde{p}(\phi) \geq 0$ . In particular,  $\tilde{Z} \geq 0$ .

Proof of the claim is provided below. It revolves around two physical points: (i) For the boson  $\phi$ , we only use the fact that all boundary conditions, and those in Eq.(22) in particular, are locally invisible. (ii) For the fermion  $\psi$ , the local invisibility of boundary conditions does not suffice, and the important point is that translations do not act on internal degrees of freedom, and therefore correspond to permutations of the lattice sites. The same holds for the half translation  $T_R$ . This distinguishes translations from internal symmetries, as well as from all other spatial symmetries, which involve point group elements, and generically act non-trivially on internal degrees of freedom. For example, a  $C_4$  rotation will act non-trivially on spin-full fermions.

*Proof:* We first consider the fermionic part of the Boltzmann weight,  $\text{Det}(I + U_\phi)$ . The Hamiltonian  $h_{\phi(\tau)}$  depends on the values of  $\phi$  at a single time slice  $\tau$ , and is therefore unaffected by the twist in bosonic boundary conditions. It follows that  $U_\phi$  is independent of the twist in bosonic boundary conditions. On the other hand, the fermionic boundary conditions in (22) correspond to a change of the time evolution operator  $U_\phi \mapsto T_R U_\phi$ , in analogy with (23). Since the  $\mathcal{C}_U$  is on-site, and  $T_R = O^{(\sigma)}$  is a permutation operator, with  $\sigma : (x, y) \mapsto (x + \Theta(y), y)$ , we have  $T_R U_\phi \in \mathcal{C}_U$ , and  $\text{Det}(I + T_R U_\phi) \geq 0$ .

Let us now consider the bosonic part of the Boltzmann weight  $e^{-S_\phi}$ , where each of the local terms  $S_{\phi;\tau,\mathbf{x}}$  is manifestly real valued for all  $\phi$ . We assume that the imaginary time circle  $S_\beta^1$  is discretized, such that the total number of space-time points  $(\tau, \mathbf{x}) = u \in U$  is finite. Such a discretization is common in DQMC algorithms [19, 21], and the continuum case can be obtained by taking the appropriate limit. The term  $S_{\phi;\tau,\mathbf{x}}$  can then be written as a composition  $f \circ g_V$ , where  $f$  is a real valued function, and  $g_V : (\phi_u)_{u \in U} \mapsto (\phi_u)_{u \in V}$  chooses the values of  $\phi$  on which  $S_{\phi;\tau,\mathbf{x}}$  depends, where  $V \subset U$  is the support of  $S_{\phi;\tau,\mathbf{x}}$ . The bosonic boundary conditions (22) then amount to a modification of the support  $V \mapsto V_\lambda$ , as depicted in Fig.6, but not of the function  $f$ , which remains real valued. In particular, for  $\lambda = 1$  we have  $S_{\phi;\tau,\mathbf{x}} \mapsto \tilde{S}_{\phi;\tau,\mathbf{x}} = f \circ g_{V_1}$ , and  $S_\phi \mapsto \tilde{S}_\phi = \sum_{\tau,\mathbf{x}} \tilde{S}_{\phi;\tau,\mathbf{x}} \in \mathbb{R}$ . Combining the above conclusions for the bosonic and fermionic parts of  $\tilde{p}(\phi) = e^{-\tilde{S}_\phi} \text{Det}(I + T_R U_\phi)$ , we find that  $\tilde{p}(\phi) \geq 0$  for all  $\phi$ .

## VI. EXCLUDING SIGN-FREE DQMC FOR CHIRAL TOPOLOGICAL MATTER

We are now ready to demonstrate the existence of an intrinsic sign problem in chiral topological matter comprised of bosons *and* fermions, using the machinery of Sections III-V.

<sup>7</sup> For  $r_0$ -local  $\phi$ , which is defined on links, plaquettes, etc., we also remove from the functional  $\phi$  integration those links, plaquettes, etc. which overlap  $l$ .



Note the close analogy between Eq.(24) and the momentum polarization (3), where the microscopic Dehn-twist  $\mathbf{T}_m$  on the torus and the half translation  $T_R$  on the cylinder play a similar role, and non-universal extensive contributions are followed by sub-extensive universal data. To make this analogy clearer, and make contact with the analysis of Sections III and VI, we consider the object  $Z_{\mathbf{T}} = \text{Tr}(\mathbf{T}_m e^{-\beta H})$ , which satisfies

$$Z_{\mathbf{T}} = Z e^{-\alpha_{\mathbf{T}} A + o(A^{-1})} \text{Tr}(\mathbf{T}), \quad (25)$$

and can be interpreted as either the (unnormalized) thermal expectation value of  $\mathbf{T}_m$ , or the partition function on a space-time twisted by  $\mathbf{T}$ , in analogy with Sec.II C. Equation (25) is valid for temperatures  $\Delta E \ll 1/\beta \ll E_g$ , much lower than the bulk gap  $E_g$  and much higher than any finite size splitting in the ground state-subspace,  $\Delta E = o(A^{-1})$ .

Just like  $T_R$ , the operator  $\mathbf{T}_m$  acts as a permutation of the lattice sites. Therefore, following Sections III and VI, if  $H$  is either locally stoquastic, or admits a locally sign-free DQMC simulation, then  $\text{Tr}(\mathbf{T}) \geq 0$ . In terms of  $c$  and  $\{\theta_a\}$ , this implies  $e^{-2\pi ic/24} \sum_a \theta_a = \text{Tr}(\mathbf{T}) \geq 0$ , where the sum runs over all topological spins.

The last statement applies to both bosonic and fermionic Hamiltonians. For bosonic Hamiltonians, it can be strengthened by means of the Frobenius-Perron theorem. If  $H' = U H U^\dagger$  is stoquastic in the on-site basis  $|s\rangle$ , Hermitian, and has a degenerate ground state subspace, then this subspace can be spanned by an orthonormal basis  $|i'\rangle$  with positive entries in the on-site basis,  $\langle s | i' \rangle \geq 0$ , see e.g. Ref.[38]. This implies that

$$0 \leq \langle i' | \mathbf{T}_m | j' \rangle = e^{-\alpha'_{\mathbf{T}} A + o(A^{-1})} \mathbf{T}_{i'j'}, \quad (26)$$

where  $\alpha'_{\mathbf{T}}$  is generally different from  $\alpha_{\mathbf{T}}$ , but the matrix  $\mathbf{T}_{i'j'}$  has the same spectrum as  $\mathbf{T}_{ij}$  in Eq.(24). This is a stronger form of (25), which implies  $\mathbf{T}_{i'j'} \geq 0$ . Since  $\mathbf{T}_{i'j'}$  is also unitary, it is a permutation matrix,  $\mathbf{T}_{i'j'} = \delta_{i', \sigma(j')}$  for some  $\sigma \in S_N$ , where  $N$  is the number of ground states. In turn, this implies that the spectrum of  $\mathbf{T}$  is a disjoint union of complete sets of roots of unity,

$$\left\{ \theta_a e^{-2\pi ic/24} \right\}_{a=1}^N = \text{Spec}(\mathbf{T}) = \bigcup_{k=1}^K R_{n_k}, \quad (27)$$

where  $R_{n_k}$  is the set of  $n_k$ th roots of unity,  $n_k, K \in \mathbb{N}$ , and  $\sum_{k=1}^K n_k = N$ . Therefore,

**Conjecture 1:** A bosonic topological phase of matter where  $\{\theta_a e^{-2\pi ic/24}\}$  is not a disjoint union of complete sets of roots of unity, admits no local Hamiltonians which are locally stoquastic.

In particular, this implies an intrinsic sign problem whenever  $1 \notin \{\theta_a e^{-2\pi ic/24}\}$ , thus generalizing Result 1. Moreover, the above statement applies non-trivially to phases with  $c \in 24\mathbb{Z}$ . In particular, for non-chiral phases, where

$c = 0$ , it reduces to the result established in Ref.[38], thus generalizing it as well. The simplest example for a non-chiral phase with an intrinsic sign problem is the doubled semion phase, where  $\{\theta_a\} = \{1, i, -i, 1\}$  [37].

Though we are currently unaware of an analog of the Frobenius-Perron theorem that applies to DQMC, we expect that an analogous result can be established for fermionic Hamiltonians.

**Conjecture 1F:** A topological phase of matter where  $\{\theta_a e^{-2\pi ic/24}\}$  is not a complete set of roots of unity, admits no local fermion-boson Hamiltonians for which locally sign-free DQMC simulation is possible.

The above conjectures suggest a substantial improvement over the criterion  $e^{2\pi ic/24} \notin \{\theta_a\}$ . To demonstrate this, we go back to the  $1/q$  Laughlin phases and  $SU(2)_k$  Chern-Simons theories considered in Table I. We find a conjectured intrinsic sign problem in *all* of the first one-thousand bosonic Laughlin phases ( $q$  even), fermionic Laughlin phases ( $q$  odd), and  $SU(2)_k$  Chern-Simons theories. In particular, we note that the prototypical  $1/3$  Laughlin phase is not captured by the criterion  $e^{2\pi ic/24} \notin \{\theta_a\}$ , but is conjectured to be intrinsically sign-problematic.

## VIII. DISCUSSION AND OUTLOOK

In this paper we established the existence of intrinsic sign problems in a broad class of chiral topological phases, namely those where  $e^{2\pi ic/24}$  does not happen to be the topological spin of an anyon. Since these intrinsic sign problems persist even when chirality, or time reversal symmetry breaking, appears spontaneously, they are rooted in the macroscopic and observable data  $c$ ,  $\{\theta_a\}$ , rather than the microscopic absence (or presence) of time reversal symmetry. Going beyond the simple setting of stoquastic Hamiltonians, we provided the first treatment of intrinsic sign problems in fermionic systems. In particular, we constructed a general framework which describes all DQMC algorithms and fermionic design principles that we are aware of, including the state of art design principles [18, 22–24] which are only beginning to be used by practitioners. Owing to its generality, it is likely that our framework will apply to additional design principles which have not yet been discovered, insofar as they are applied locally. We also presented conjectures that strengthen our results, and unify them with those obtained in Refs.[9, 38], under a single criterion in terms of  $c$  and  $\{\theta_a\}$ . These conjectures also imply intrinsic sign problems in many topological phases not covered by existing results.

Conceptually, our results show that the sign problem is not *only* a statement of computational complexity: it is, in fact, intimately connected with the physically observable properties of quantum matter. Such a connection has long been heuristically appreciated by QMC practitioners, and is placed on a firm and quantitative footing by the discovery of intrinsic sign problems.

Despite the progress made here, our understanding of intrinsic sign problems is still in its infancy, and many open questions remain:

*Quantum computation and intrinsic sign problems* Intrinsic sign-problems relate the physics of topological phases to their computational complexity, in analogy with the classification of topological phases which enable universal quantum computation [48, 49]. As we have seen, many phases of matter that are known to be universal for quantum computation are also intrinsically sign-problematic, supporting the paradigm of ‘quantum advantage’ or ‘quantum supremacy’ [50]. Determining whether intrinsic sign-problems appear in *all* phases of matter which are universal for quantum computation is an interesting open problem. Additionally, we identified intrinsic sign problems in many topological phases which are not universal for quantum computation. The intermediate complexity of such phases between classical and quantum computation is another interesting direction for future work.

*Unconventional superconductivity and intrinsic sign problems* As described in the introduction, a major motivation for the study of intrinsic sign problems comes from long standing open problems in fermionic many-body systems, the nature of high temperature superconductivity in particular. It is currently believed that many high temperature superconductors, and the associated repulsive Hubbard models, are *non-chiral*  $d$ -wave superconductors [17, 27], in which we did not identify an intrinsic sign problem. The optimistic possibility that the sign problem can in fact be cured in repulsive Hubbard models is therefore left open, though this has not yet been accomplished in the relevant regime of parameters, away from half filling, despite intense research efforts [26]. Nevertheless, the state of the art DMRG results of Ref.[27] do not exclude the possibility of a *chiral*  $d$ -wave superconductor ( $\ell = \pm 2$  in Table I). In this case we do find an intrinsic sign problem, which would account for the notorious sign problems observed in repulsive Hubbard models. More speculatively, it is possible that the mere proximity of repulsive Hubbard models to a chiral  $d$ -wave phase stands behind their notorious sign problems. The possible effect of an intrinsic sign problem in a given phase on the larger phase diagram was recently studied in Ref.[111]. There is also evidence for chiral  $d$ -wave superconductivity in doped graphene and related materials [112, 113], and our results therefore suggest the impossibility of sign-free QMC simulations of these. We believe that the study of intrinsic sign problems in the context of unconventional superconductivity is a promising direction for future work.

*Non-locality as a possible route to sign-free QMC* The intrinsic sign problems identified in this work add to existing evidence for the complexity of chiral topological phases - these do not admit local commuting projector Hamiltonians [54, 114–116], nor do they admit local Hamiltonians with a PEPS state as an exact ground state [43, 117–119].

Nevertheless, relaxing the locality requirement does lead

to positive results for the simulation of chiral topological matter using commuting projectors or PEPS. First, commuting projector Hamiltonians can be obtained if the local bosonic or fermionic degrees of freedom are replaced by anyonic (and therefore non-local) excitations of an underlying chiral topological phase [120]. Second, chiral topological Hamiltonians can have a PEPS ground state if they include interactions (or hopping amplitudes) that slowly decay as a power-law with distance.

One may therefore hope that sign-free QMC simulations of chiral topological matter can also be performed if the locality requirements made in Sec.V are similarly relaxed. Do such ‘weakly-local’ sign-free models exist?

*Easing intrinsic sign problems* In this paper we proved the existence of an intrinsic sign problem in chiral topological phases of matter, but we did not quantify the *severity* of this sign problem, which is an important concept in both practical applications and theory of QMC. The severity of a sign problem is quantified by the smallness of the average sign,  $\langle \text{sgn} \rangle := \sum p / \sum |p|$ , of the QMC weights  $p$  with respect to the distribution  $|p|$ . Since  $\langle \text{sgn} \rangle$  can be viewed as the ratio of two partition functions, it obeys the generic scaling  $\langle \text{sgn} \rangle \sim e^{-\Delta \beta N}$ , with  $\Delta \geq 0$ , as  $\beta N \rightarrow \infty$  [2, 10]. A sign problem exists when  $\Delta > 0$ , in which case QMC simulations require exponential computational resources, and this is what the intrinsic sign problem we identified implies for ‘most’ chiral topological phases of matter. From the point of view of computational complexity, all that matters is whether  $\Delta = 0$  or  $\Delta > 0$ , but for practical applications the value of  $\Delta$  is very important, see e.g [112]. One may hope for a possible refinement of our results that provides a lower bound  $\Delta_0 > 0$  for  $\Delta$ , but since we have studied *topological* phases of matter, we view this as unlikely. It may therefore be possible to obtain fine-tuned models and QMC methods that lead to a  $\Delta$  small enough to be *practically* useful. More generally, it may be possible to search for such models algorithmically, thus *easing* the intrinsic sign problem [10, 121].

*Possible extensions* The chiral central charge only appears modulo 24 in our results. Nevertheless, the full value of  $c$  is physically meaningful, as reviewed in the introduction. Does an intrinsic sign problem exist in all phases with  $c \neq 0$ ? The results of Ref.[39] strongly suggest this.

The arguments of Ref.[38] and Sec.VII apply equally well to any element of the modular group, rather than just the topological  $\mathbf{T}$ -matrix, implying that the spectrum of all elements decomposes into full sets of roots of unity. This may imply a more restrictive constraint on the TFT data than conjectured in Sec.VII.

It is believed that all SPT phases can be characterized by universal complex phases acquired by their partition functions, when placed on certain non-trivial space-times [122–126], in analogy with Eq.(3). Loosely speaking, for an SPT with on-site symmetry group  $G$ , the relevant space-time would be obtained by purely geometric manipulations as performed in this paper, along with a twisting of boundary



conditions by elements  $g \in G$ . Since each  $G$  acts on-site, we do not expect intrinsic sign problems whenever a non-trivial  $g$  is required to detect the SPT [127–130]. Nevertheless, it may be possible to obtain weaker statements, constraining the possible bases in which a Hamiltonian in a  $G$ -SPT may be stoquastic. Such constraints may be more useful for designing sign-free models than the stronger intrinsic sign problems discussed in this paper. Similar questions arise in the context of topologically ordered phases, enriched by an on-site symmetry.

Finally, going beyond gapped topological phases, are there intrinsically sign-problematic phases which are not gapped, not topological, or both? It is the authors' hope that answers to some of these questions will shed new light on the formidable quantum many-body problem.

## ACKNOWLEDGMENTS

O.G. is grateful to his wife Adi Cohen-Golan, for her invaluable support in the completion of this work during the Coronavirus lockdown in Israel. We thank Ryan Thorngren for participation in early stages of this work and feedback on the manuscript, and Snir Gazit for providing the much needed practitioner's point of view on DQMC and the sign problem. We also benefited from discussions with Ady Stern, Ari Turner, Ciarn Hickey, Erez Berg, Eyal Cornfeld, Eyal Leviatan, Johannes Stephan Hofmann, Michael Levin, Paul Wiegmann, and Raquel Queiroz. This work was supported by the Israel Science Foundation (ISF, 2250/19), the Deutsche Forschungsgemeinschaft (DFG, German Research Foundation, CRC/Transregio 183, EI 519/7-1), and the European Research Council (ERC), under Project LEGOTOP and the European Union's Horizon 2020 research and innovation program (grant agreement No. 771537).

## Appendix A: Further details regarding Eq.(3)

This appendix involves basic facts in CFT, which can be found in e.g [83, 84].

### 1. Definition of $h_0$ and ambiguities in its value

A chiral topological phase of matter has a finite-dimensional ground state subspace on the spatial torus. A basis  $\{|a\rangle\}_{a=1}^N$  for the torus ground state subspace exists, such that each state  $|a\rangle$  corresponds to a conformal family in the boundary CFT [40, 41, 107], constructed over a primary with right/left moving conformal weights  $h_a^{(l)}, h_a^{(r)} \geq 0$ . The corresponding chiral and total conformal weights are then given by  $h_a = h_a^{(l)} - h_a^{(r)}$  and  $h_a^+ = h_a^{(l)} + h_a^{(r)}$ , respectively. The chiral and total central charges of the CFT are similarly defined in terms of

the left/right moving central charges,  $c = c^{(l)} - c^{(r)}$  and  $c^+ = c^{(l)} + c^{(r)}$ .

When the torus is cut to a cylinder with finite circumference  $L$ , the ground state degeneracy is lifted, generically leaving a unique ground state. The lowest energy eigenstates on the cylinder can also be labeled as  $\{|a\rangle\}_{a=1}^N$ . Each  $|a\rangle$  corresponds to a non-universal choice of state in the conformal family labeled by  $h_a^{(l)}, h_a^{(r)}$ , which need not be the primary, as demonstrated explicitly in Appendix B below.

If the boundary is described by an idealized CFT, all  $|a\rangle$ s correspond to primaries, and the corresponding energies are given by  $E_a = (4\pi v/L)(h_a^+ - c^+/24)$ , relative to the ground state energy on the torus, where  $v$  is the velocity of the CFT and  $L$  is the circumference of the cylinder. These expressions receive exponentially small corrections of  $O(L e^{-R/\xi})$  and  $O(R e^{-L/\xi})$ , where  $\xi$  is the bulk correlation length and  $R$  is the length of the cylinder [79]. The cylinder ground state then corresponds to the CFT ground state, the primary with minimal  $h_a^+$ .

More generally, each state  $|a\rangle$  corresponds to either a primary or a descendent, and has conformal weights  $h_a^{(l)} + n_a^{(l)}, h_a^{(r)} + n_a^{(r)}$ , where  $n_a^{(l)}, n_a^{(r)} \in \mathbb{N}_0$ . The corresponding energies  $E_a$  differ from the idealized  $(4\pi v/L)(h_a^+ - c^+/24)$ , and the choice of conformal family  $a_0$  with minimal  $E_{a_0}$  is non-universal. In terms of  $n_a = n_a^{(l)} - n_a^{(r)}$ , we then define  $h_0 := h_{a_0} + n_{a_0}$ , the chiral conformal weight associated with the cylinder ground state  $|a_0\rangle$ . The value of  $h_0$  therefore carries two ambiguities: a choice of conformal family  $a_0 \in \{a\}$ , and the choice of a state in the conformal family,  $n_{a_0} \in \mathbb{N}_0$ . As described in Sec.IIB, the only universal statement is  $\theta_0 = e^{2\pi i h_0} \in \{\theta_a\}$ , where  $\theta_a = e^{2\pi i h_a}$  are the topological spins of bulk anyons.

The result of Ref.[40] for the momentum polarization is given terms of the low lying cylinder eigenstates  $|a\rangle$ ,

$$\langle a | T_R | a \rangle = \exp \left[ \alpha N_x + \frac{2\pi i}{N_x} \left( h_a - \frac{c}{24} \right) + o(N_x^{-1}) \right], \quad (\text{A1})$$

where the lattice spacing is set to 1,  $N_x = L$ . It follows that the thermal expectation value  $\tilde{Z}/Z = \text{Tr}(T_R e^{-\beta H})/Z$  is equal to  $\exp \left[ \alpha N_x + \frac{2\pi i}{N_x} \left( h_0 - \frac{c}{24} \right) + o(N_x^{-1}) \right]$ , if the temperature  $\beta^{-1}$  is much lower than the boundary energy differences  $\sim N_x^{-1}$ , namely  $\beta^{-1} = o(N_x^{-1})$ , as described in Sec.II.

### 2. The value of $h_0$ in fermionic phases of matter

Fermionic topological phases are microscopically comprised of fermions (and possibly bosons), and have the fermion parity  $(-1)^{N_f}$  as a global symmetry [47, 123, 131, 132]. It is therefore useful to probe such phases with a background  $\mathbb{Z}_2$  gauge field corresponding to  $(-1)^{N_f}$ , or a

spin structure. For our purposes, this amounts to considering both periodic and anti-periodic boundary conditions around non-contractible cycles in space-time.

In the main text we were only interested in locally sign-free QMC representations of thermal partition functions, and sign-free geometric manipulations that can be performed to these. We therefore restricted attention to thermal boundary conditions in the imaginary time direction (see Sec. V A), and to periodic boundary conditions around the spatial cylinder. These boundary conditions cannot generically be modified without introducing signs into the QMC weights.

Here we provide a fuller picture by considering the behavior of  $h_0$  with both periodic and anti-periodic boundary conditions, in the closed  $x$  direction of the spatial cylinder. Since  $h_0$  is a ground state property, the time direction is open and does not play a role.

For a fermionic chiral topological phase, the boundary CFT is also fermionic. The primary conformal weights  $\{h_a\}$  then depend on the choice of boundary conditions (in the  $x$  direction), and as a result, so will the set of topological spins  $\{\theta_a\}$  in which  $\theta_0 = e^{2\pi i h_0}$  is valued. In particular, the vacuum spin  $\theta_I = 0$  will not be included in  $\{\theta_a\}$  for periodic boundary conditions, while for anti-periodic boundary conditions, both the vacuum  $\theta_I = 1$  and the spin  $\theta_\psi = -1$  of the microscopic fermion will appear [41, 83]. Note that  $\theta_\psi$  does not correspond to an emergent fermion, as in e.g the toric code [133], and therefore does not imply an additional ground state on the torus.

As an example, consider the series of Laughlin phases at filling  $1/q$ , with  $q \in \mathbb{N}$ , all of which have the chiral central charge  $c = 1$ . First, for  $q \in 2\mathbb{N}$  the phase is bosonic, and we consider only periodic boundary conditions. The primary conformal weights are given by  $h_a = a^2/2q$  [36, 134], with  $a \in \mathbb{N}_0$ . The topological spins  $\theta_a = e^{2\pi i h_a}$  depend only on  $a \bmod q$ , and the  $q$  spins  $\{\theta_a\}_{a=0}^{q-1}$  (appearing in Table I) correspond to the  $q$  degenerate ground states on the torus. In particular, the vacuum spin  $\theta_I = 1$  is obtained for  $a = 0$ .

For  $q \in 2\mathbb{N} - 1$  the phase is fermionic, and we consider both periodic and anti-periodic boundary conditions. For periodic boundary conditions the weights are given by  $h_a = (a + 1/2)^2/2q$  [36]. As in the bosonic case,  $\theta_a = e^{2\pi i h_a}$  depend only on  $a \bmod q$ , with  $\{\theta_a\}_{a=0}^{q-1}$  (appearing in Table I) corresponding to the  $q$  degenerate ground states on the torus. Unlike the bosonic case, the vacuum spin  $\theta_I = 1$  is not included in  $\{\theta_a\}_{a=0}^{q-1}$ . For anti-periodic boundary conditions, the weights are given by  $h_a = a^2/2q$  as in the bosonic case [134]. The set  $\{\theta_a\}_{a=0}^{q-1}$  again corresponds to the  $q$  torus ground states, but now  $\theta_\psi = \theta_{a=q} = -1$  is an additional topological spin that corresponds to the physical Fermion  $\psi$  [68].

The simplest fermionic Laughlin phase is given by  $q = 1$ , and corresponds to a Chern insulator with Chern number  $\nu = 1$  [85, 86], which is studied in detail in Appendix B below. The Chern insulator has a unique ground state on the torus, and accordingly, there is a unique topological

spin  $\theta_\sigma = e^{2\pi i(1/8)}$  for periodic boundary conditions on the cylinder, and two topological spins  $\theta_I = 1, \theta_\psi = -1$  for anti-periodic boundary conditions. Here  $\psi$  corresponds the physical fermions from which the Chern insulator is comprised. The object carrying the spin  $\theta_\sigma$  is the complex analog of the celebrated Majorana zero mode supported on vortices in the bulk of a  $p + ip$  superconductor [46, 52].

## Appendix B: Momentum polarization with non CFT boundaries

As reviewed in Sec. II, the existing analytic derivation of Eq. (3) relies on the CFT description of the physical boundaries of the cylinder, and of the line  $y = 0$  where  $T_R$  is discontinuous [40]. In this appendix we perform an analytic and numerical study that shows that, at least for free fermions, the relevant CFT expressions and the resulting Eq. (3), hold even if the boundary is not described by an idealized CFT. We will however, find a number of subtleties which have not been demonstrated in the literature, as already described below Eq. (2) and in Appendix A.

### 1. CFT finite-size correction in non CFT boundaries

The main ingredient in the analytic derivation of Eq. (3) is the expression (2) for the finite size correction to the momentum density in CFT [40]. In this appendix we show that, at least in the non-interacting case, Equation (2) remains valid, with  $\theta_0 = e^{2\pi i h_0} \in \{\theta_a\}$ , even when the boundary cannot be described by a CFT.

We will consider a Chern insulator, such as the prototypical Haldane model [85]. When the boundary degrees of freedom can be described by a CFT, they correspond to the Weyl fermion CFT, where  $c = \pm 1$  and the primary conformal weights are  $h_\sigma = \pm 1/8$  ( $h_I = 0, h_\psi = \pm 1/2$ ) for periodic (anti-periodic) boundary conditions, as described in Appendix A 2. The sign corresponds to the two possible chiralities. More generally, on a lattice with spacing 1, the boundary supports a complex fermion with an energy dispersion  $\varepsilon_k$ , where  $k = k_x$  takes values in the Brillouin zone  $\mathbb{R}/2\pi\mathbb{Z}$  for an infinite circumference  $L = \infty$ , or its discretization  $(2\pi/L)\mathbb{Z}_L$  ( $(2\pi/L)(\mathbb{Z}_L + 1/2)$ ), for  $L < \infty$  and periodic (anti-periodic) boundary conditions. The only requirement on  $\varepsilon_k$  is that it be *chiral*, in the sense that it connects the two separated bulk energy bands. If the intersections  $k_l$  and  $k_u$  with the lower and upper bulk bands, respectively, satisfy  $k_l < k_u$  ( $k_l > k_u$ ), we say that the boundary is right (left) moving, or has a positive (negative) chirality, see Fig. 7.

More generally, the dispersion will contain several dispersion branches  $\{\varepsilon_{j,k}\}_{j=1}^J$ , but since the momentum density is additive in  $j$  we restrict attention to a single branch. Without loss of generality, we also fix the chemical potential  $\mu = 0$ , in which case the Fermi momentum  $k_F$  satisfies

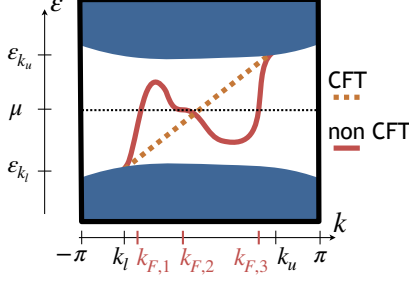


FIG. 7. Schematic band structure, energy  $\varepsilon$  as a function of momentum  $k = k_x$  in the periodic  $x$  direction, of a Chern insulator on the cylinder. The figure shows the bulk energy bands (blue) and the chiral boundary dispersion, with two dispersion branches, on a single boundary component (orange and red curves). The opposite chirality branches on the second boundary component are not drawn. The momenta  $k_l$  and  $k_u$  correspond to the intersections of the boundary dispersion with the lower and upper bulk bands, respectively. Since  $k_u > k_l$ , both dispersion branches have a positive chirality. The orange line indicates the idealized linear dispersion with a single Fermi momentum  $k_F = 0$ , which corresponds to the Weyl fermion CFT. The solid red curve corresponds to a more general chiral branch, with three Fermi momenta  $k_{F,1}, k_{F,2}, k_{F,3}$ , where the dispersion around  $k_{F,2}$  takes a (non-generic) non-linear form. With periodic boundary conditions around the cylinder, both dispersion branches produce the same  $L^{-2}$  correction to the momentum density in Eq.(B2), with a positive chirality  $+$ , up to a mod 1 ambiguity:  $1/12 \mapsto 1/12 + n$ ,  $n \in \mathbb{N}$ .

$\varepsilon_{k_F} = 0$ . The value of  $k_F$  plays an important role in the subsequent analysis.

The simplest dispersion that satisfies the above requirements is the linear one  $\varepsilon_k = v(k - k_F)$ . For  $k_F = 0$  this corresponds to the Weyl fermion CFT. The presence of  $k_F \neq 0$  corresponds to the addition of a chemical potential  $vk_F$ , which breaks the conformal symmetry. The generic form is  $\varepsilon_k = v(k - k_F) + O(k - k_F)^2$ . A non-generic dispersion can take the form  $\varepsilon_k = v_3(k - k_F)^3 + O(k - k_F)^4$ , and there may be several Fermi momenta if the dispersion is non monotonic, see Fig.7.

In all cases the many-body ground state momentum is given by summing the momenta of all filled single Fermion states  $p(L) = \frac{1}{L} \sum_{\varepsilon_k < 0} k$ , where the sum runs over  $k \in (2\pi/L)\mathbb{Z}_L$  such that  $\varepsilon_k$  is negative and in the bulk energy gap. In order to obtain  $p$  as a continuous function of  $L$ , we treat the bulk energy gap as a smooth cutoff  $p(L) = \frac{1}{L} \sum_{\varepsilon_k < 0} kC(\varepsilon_k)$ , where the function  $C(\varepsilon)$  goes to 1 (0) fast enough as  $\varepsilon$  goes to 0 ( $\varepsilon_{k_l}$  or  $\varepsilon_{k_u}$ )<sup>8</sup>. The cutoff  $C$  represents the smooth delocalization of boundary eigenstates as their energy nears the bulk energy bands.

To obtain the  $L$  dependence of  $p(L)$ , we will use the

Euler-Maclaurin formula

$$\sum_{n=n_1}^{n_2} f(n) = \int_{n_1}^{n_2} f(x) dx + \frac{f(n_2) + f(n_1)}{2} + \frac{1}{6} \frac{f'(n_2) - f'(n_1)}{2!} - \frac{1}{30} \frac{f'''(n_2) - f'''(n_1)}{4!} + R, \quad (\text{B1})$$

where the remainder satisfies  $|R| \leq \frac{2\zeta(5)}{(2\pi)^5} \int_{n_1}^{n_2} |f^{(5)}(x)| dx$ . We begin by considering periodic boundary conditions, where we set  $f(n) = (2\pi n/L^2) C(\varepsilon_{2\pi n/L})$ . Assuming a single, vanishing, Fermi momentum  $k_F = 0$ , we set  $(n_1, n_2) = (-\infty, 0)$  for positive chirality, and  $(n_1, n_2) = (0, \infty)$  for negative chirality. Equation (B1) then gives

$$p(L) = p(\infty) \pm \frac{2\pi}{L^2} \frac{1}{12} + O\left(\frac{1}{L^4}\right), \text{ as } L \rightarrow \infty, \quad (\text{B2})$$

where  $p(\infty) = \int_{\varepsilon_k < 0} kC(\varepsilon_k) dk/2\pi$  and  $\pm = \text{sgn}(k_u - k_l)$  is the chirality. The  $1/L^2$  correction in (B2) comes from  $f'(0) = 2\pi/L^2$  in (B1). We see that the leading finite size correction  $h_0 - c/24$  is unchanged from its CFT value  $h_\sigma - c/24 = \pm 1/12$ , even when a CFT description does not apply.

The case of a single non-zero Fermi momentum  $k_F \neq 0$  is more interesting, as it demonstrates that the integer part of  $h_0$  can change as a function of  $L$  and  $k_F$ . The direct derivation of the end result from the Euler-Maclaurin formula is surprisingly lengthy, so we omit it and present a more direct route to the end result. To be concrete, assume a positive chirality and  $k_F > 0$ . The Euler-Maclaurin formula leads to cutoff independent results, so we can restrict attention to cutoff functions  $C(\varepsilon_k)$  which are identically 1 for  $0 < k < k_F$ . Since these can serve as cutoff functions for the case  $k_F = 0$  as well, we can deduce the  $k_F \neq 0$  momentum density  $p(L, k_F)$  from the  $k_F = 0$  momentum density  $p(L)$ ,

$$\begin{aligned} p(L, k_F) &= \frac{1}{L} \sum_{k < k_F} kC(\varepsilon_k) \\ &= \frac{1}{L} \sum_{k < 0} kC(\varepsilon_k) + \frac{1}{L} \sum_{0 < k < k_F} k \\ &= p(L) + \frac{2\pi}{L^2} \sum_{l=1}^n l, \end{aligned} \quad (\text{B3})$$

where  $n = \lfloor k_F L/2\pi \rfloor$ . Using Eq.(B2), we then have

$$p(L, k_F) = p(\infty) + \frac{2\pi}{L^2} \left[ \frac{1}{12} + \sum_{l=1}^n l \right] + O\left(\frac{1}{L^4}\right), \quad (\text{B4})$$

where  $p(\infty)$  is the momentum density at  $L = \infty$  and  $k_F = 0$ . We see that the value of  $h_0 - c/24$  is only equal to the idealized CFT result  $h_\sigma - c/24 = 1/12$  modulo 1, while the integer part jumps periodically as a function of  $k_F$  at

<sup>8</sup> It suffices that  $C'(\varepsilon)$  vanish at  $\varepsilon = 0, \varepsilon_{k_l}, \varepsilon_{k_u}$ .

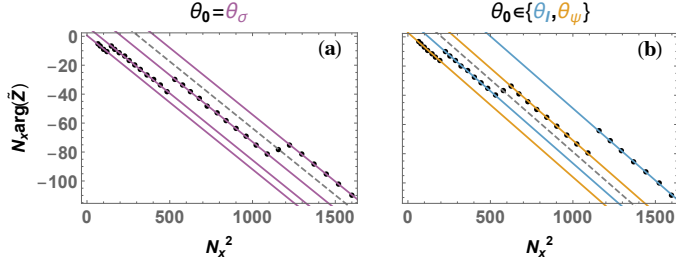


FIG. 8. Numerical results for the momentum polarization Eq.(3), in a Chern insulator with  $k_F \neq 0$ . Black dots mark numerically obtained values of  $N_x \arg \tilde{Z}$  as a function of  $N_x^2$ . (a) Periodic boundary conditions. Purple lines indicate linear fits, with approximately the same slope and intercepts  $2\pi(1/12 + \sum_{l=1}^n l)$  with the  $y$  axis, with  $n = 0, 1, 2, 3$ , in accordance with Eq.(B4). This allows for the extraction of the topological spin  $\theta_\sigma = e^{2\pi i(1/8)}$ . To illustrate the possibility of accidental degeneracies, we choose  $k_F = 3/34$ , where a degeneracy occurs for  $N_x = 34$ , and the average value of  $N_x \arg \tilde{Z}$  between the two ground states is obtained. A grey dotted line indicates the average of the two neighboring purple lines. (b) Anti-periodic boundary conditions. Colored lines indicate linear fits, with approximately the same slope, and intercepts  $2\pi[-1/24 + \sum_{l=1}^n (l - 1/2)]$ , with  $n = 1, 2, 3, 4$ , in accordance with Eq.(B5). The value  $n = 0$  is not obtained as it occurs only for small circumferences  $N_x < 6$  where  $N_x \arg \tilde{Z}$  is not computed. Orange lines correspond to the fermion spin  $\theta_\psi = -1$ , while blue lines correspond to the vacuum spin  $\theta_I = 0$ . To illustrate the possibility of accidental degeneracies, we choose  $k_F = (5/2)/24$ , where an accidental degeneracy occurs for  $N_x = 24$ .

fixed number of sites  $L$ , or as the number of sites  $L$  at fixed  $k_F$ . Treating  $k_F$  as fixed and valued in  $(-\pi, \pi]$ , the period in  $L$  is given by  $q = |2\pi/k_F| \geq 2$ , which need not be an integer. As described in Appendix A, the mod 1 ambiguity is attributed to  $h_0$  rather than  $c$ , which corresponds to the topological spin  $\theta_0 = \theta_\sigma = e^{2\pi i(1/8)}$ .

The interpretation of Eq.(B4) is straight forward. As the number of sites  $L$  increases, the single particle momenta  $(2\pi/L)\mathbb{Z}_L$  become denser in the Brillouin zone  $\mathbb{R}/2\pi\mathbb{Z}$ . The  $n$ th jump in  $h_0$  correspond to the motion of a single particle state with momentum  $2\pi n/L$  through  $k_F$  and into the Fermi sea, adding a momentum density  $2\pi n/L^2$  to the ground state.

Figure 8 presents the results of numerical computations of the momentum polarization Eq.(3) in a Chern insulator with  $k_F \neq 0$  on a square lattice. Details of the model and computations can be found in the accompanying Mathematica notebook. In particular, Fig.8(a) verifies Eq.(B4).

A subtle point, not mentioned above, is that when  $k_F L/2\pi \in \mathbb{Z}$ , which happens only when  $k_F/2\pi = a/b$  is rational and  $L \in b\mathbb{N}$ , a single particle state with momentum exactly  $k_F$  exists, leading to an accidental degeneracy on the cylinder, between two many-body ground states with momentum densities given by Eq.(B4) with  $n$  and  $n+1$ . The momentum polarization (3) then gives the average mo-

mentum density in the two ground-states, as visualized by the grey dotted line in Fig.8(a). For such system sizes the value  $\theta_0 = -\theta_\sigma$  may be obtained rather than the generic  $\theta_0 = \theta_\sigma$ .

The same analysis can be performed for anti-periodic boundary conditions, where we sum over single particle momenta  $k \in \frac{2\pi}{L}(\mathbb{Z}_L + \frac{1}{2})$ . Equation (B4) is then modified to

$$p(L, k_F) = p(\infty) + \frac{2\pi}{L^2} \left[ -\frac{1}{24} + \sum_{l=1}^n \left( l - \frac{1}{2} \right) \right] + O\left(\frac{1}{L^4}\right), \quad (\text{B5})$$

where  $n = \lfloor \frac{k_F L}{2\pi} - \frac{1}{2} \rfloor$ . As a function of  $L$ , jumps in  $h_0 - c/24$  occur with the same period  $q = |2\pi/k_F| \geq 2$ , but are shifted by  $q/2$ . Moreover,  $h_0 - c/24$  now attains two values modulo 1, namely  $h_I - c/24 = -1/24$  and  $h_\psi - c/24 = 1/2 - 1/24$ .

Equation (B5) therefore demonstrates explicitly the statements made in Appendix A 1. For  $k_F = 0$ , the cylinder ground state of the Chern insulator corresponds to the idealized Weyl fermion CFT. A single value  $h_0 = 0$  is attained, which is the conformal weight  $h_I$  of the CFT vacuum. A non-vanishing  $k_F$  corresponds to the addition of a chemical potential to the CFT, which changes the energies of the CFT states, favoring a CFT excited state over the CFT vacuum. The cylinder ground state of the Chern insulator may then correspond to any CFT state in the conformal family of either the vacuum  $I$  or fermion  $\psi$ , which need not be primary. From the bulk TFT perspective, we see that  $\theta_0 = e^{2\pi i h_0}$  may be equal to either of the topological spins  $\theta_I = 1, \theta_\psi = -1$  as a function of  $L$ .

As in the case of periodic boundary conditions, accidental degeneracies on the cylinder occur when  $k_F L/2\pi \in \mathbb{Z} + 1/2$ , changing the value of  $h_0$  attained from the momentum polarization to its average over the degenerate states. For such system sizes, the value  $\theta_0 = \pm \sqrt{\theta_I \theta_\psi}$  is obtained than the generic  $\theta_0 \in \{\theta_I, \theta_\psi\}$ .

Equation (B5) is verified numerically in Fig.8(b), which demonstrates that the value of  $\theta_0 = e^{2\pi i h_0}$ , obtained from the momentum polarization (3), takes different values in the set  $\{\theta_a\}$  of topological spins as a function of system size  $L$ , apart from accidental degeneracies.

## 2. No finite-size correction at finite temperature

The line  $y = 0$  where  $T_R$  jumps can be interpreted as an additional boundary component at the 'entanglement temperature'  $\beta_*^{-1}$ . Reference [40] used the modular transformations of CFT partition functions to demonstrate that when  $\beta_* \ll L/v$ , this boundary component does not contribute to the  $1/L$  correction to  $\log \tilde{Z}$ . Here, we note that the same result holds for free fermions with a general dispersion  $\varepsilon_k$ . The contribution of the additional boundary component to  $\log \tilde{Z}$  is given by  $\log \tilde{Z}_*(L) = L f_*(L)$ , with



the free energy density

$$f_*(L) = \frac{1}{L} \sum_k \log(1 + e^{iak} e^{-\beta_* \varepsilon_k}) C(\varepsilon_k). \quad (\text{B6})$$

Using Eq.(B1) one finds  $f_*(L) = f_*(\infty) + O(L^{-4})$  for both periodic and anti-periodic boundary conditions, which implies  $\log \tilde{Z}_* = L f_*(\infty) + O(L^{-3})$ , with no  $1/L$  contribution. The complex number  $f_*(\infty) = \int \log(1 + e^{iak} e^{-\beta_* \varepsilon_k}) C(\varepsilon_k) dk / 2\pi$  contributes to the non-universal  $\alpha$  in Eq.(3).

### Appendix C: Cutting the torus along an arbitrary vector

For  $\mathbf{d} = (d_x, 0)$  we restrict to  $N_x = n_x d_x$ ,  $n \in \mathbb{N}$ , viewing  $d_x$  as an enlarged lattice spacing, and treating  $n$  as a reduced number of sites along the circumference in place of  $N_x$ . The same logic applies to  $\mathbf{d} = (0, d_y)$ . For  $\mathbf{d} = (d_x, d_y)$  with both  $d_x, d_y \neq 0$ , we restrict to system sizes  $(N_x, N_y) = n\mathbf{d}$ , such that the line  $l = \text{span}_{\mathbb{R}} \mathbf{d}$  is a diagonal of the rectangle  $nN_x \times nN_y$  and corresponds to a circle on the torus  $(\mathbb{R}/N_x\mathbb{Z}) \times (\mathbb{R}/N_y\mathbb{Z})$ . Cutting  $X$  along this line produces a cylinder  $C$  of circumference  $L = n|\mathbf{d}|$ . We then view  $|\mathbf{d}|$  as a lattice spacing and  $n$  as the number of sites along the circumference. Note that the distance between the boundary components of the resulting cylinder is  $R = nd_x d_y / |\mathbf{d}|$ , and the thermodynamic limit is indeed obtained as  $n \rightarrow \infty$ . With these identifications the momentum polarization (3) remains unchanged, apart from a modification of the non-universal  $\alpha$  to  $\alpha|\mathbf{d}|^2$ .

### Appendix D: Dealing with accidental degeneracies on the cylinder

As demonstrated in Appendix B, for certain system sizes  $N_x$  accidental degeneracies occur on the cylinder, and the function  $\theta_0(N_x) = e^{2\pi i h_0(N_x)}$  obtained from Eq.(3) may take values outside the set  $\{\theta_a\}$ , namely  $\theta_0 = \pm\sqrt{\theta_a \theta_b}$  for a two-fold degeneracy. In this appendix we complete the derivation of Result 1 and 1F by considering the possibility of such degeneracies.

First, even in the presence of degeneracies,  $\theta_0$  is valued in a finite set. Therefore, Eq.(6) still implies that  $\epsilon' = n/m$  is rational, and that  $\theta_0(N_x) e^{-2\pi i c/24} = e^{-2\pi i \epsilon' N_x^2}$  periodically covers a subset  $S \ni 1$  of  $m$ th roots of unity, for all large enough  $N_x$ . We denote by  $\mathcal{N} \subset \mathbb{N}$  the set of circumferences  $N_x$  for which a degeneracy appears and  $\theta_0(N_x) \notin \{\theta_a\}$ . If circumferences  $N_x \in m\mathbb{N}$ , where  $e^{2\pi i \epsilon' N_x^2} = 1$ , are not all contained in  $\mathcal{N}$ , then  $1 = \theta_0(N_x) e^{-2\pi i c/24} \in \{\theta_a e^{-2\pi i c/24}\}$ , as stated in Results 1 and 1F.

We are left with the complementary case, where degeneracies occur for all  $N_x \in m\mathbb{N}$ , i.e  $m\mathbb{N} \subset \mathcal{N}$ . Note that

this case is highly fine tuned, as it ties together the non-universal  $\epsilon' = n/m$  and the set  $\mathcal{N}$  of  $N_x$ s where accidental degeneracies appear. In order to deal with this case, we make use of the Frobenius-Perron theorem to resolve the degenerate ground-state subspace, without introducing signs. The analysis applies only to the bosonic setting of Result 1, and is similar to that made in Sec.VII. We now have a Hamiltonian  $H'$  on the cylinder, which has an exactly degenerate ground-state subspace for all  $N_x \in m\mathbb{N}$ , and has non-positive matrix elements in the on-site homogeneous basis  $|s\rangle$ . The Frobenius-Perron theorem implies that an orthonormal basis  $|i\rangle$  with non-negative entries may be chosen for the ground state subspace,  $\langle s|i\rangle \geq 0$  for all  $s, i$ . It follows that the matrix elements of  $T_R$  in the basis  $|i\rangle$  are non-negative,  $M_{ij} := \langle i|T_R|j\rangle \geq 0$ . Taking the  $N_x$ th matrix power of  $M$  we have  $(M^{N_x})_{ij} \geq 0$ . Equation (3) implies that the eigenvalues of  $M^{N_x}$  are of the form  $e^{-\delta' N_x^2} e^{-2\pi i \epsilon' N_x^2 + o(1)} \theta_a e^{-2\pi i c/24}$ , so we can write  $(M^{N_x})_{ij} = e^{-\delta' N_x^2} e^{-2\pi i \epsilon' N_x^2 + o(1)} T_{ij}$ , where  $T_{ij}$  has eigenvalues  $\{\lambda\} \subset \{\theta_a e^{-2\pi i c/24}\}$ . In particular,  $T_{ij}$  is unitary. Since  $e^{2\pi i \epsilon' N_x^2} = 1$  for all  $N_x \in m\mathbb{N}$ , we see that  $T_{ij}$  also has non-negative entries, and is therefore a permutation matrix, containing 1 in its spectrum (see Sec.VII). It follows that  $1 \in \{\lambda\} \subset \{\theta_a e^{-2\pi i c/24}\}$ , asserting Result 1.

We are currently unaware of an analog of the Frobenius-Perron theorem in the context of DQMC, that may be used to resolve the degenerate ground-state subspace without introducing signs. Instead, we will make a physical assumption under which Result 1F holds. Namely, we will assume that the fine tuned constraint  $\epsilon' = n/m$  and  $m\mathbb{N} \subset \mathcal{N}$  may be lifted by a sign-free perturbation. This includes (i) perturbations to the effective single-fermion Hamiltonian  $h_{\phi(\tau)}$  that do not violate the algebraic condition  $h_{\phi(\tau)} \in \mathcal{C}_h$ , (ii) perturbations to the bosonic action  $S_\phi$  that maintain its reality, and (iii) changes of the vector  $\mathbf{d}$  along which the torus is cut to a cylinder, as described in Appendix C, which will generically change the details of the boundary spectrum, including the non-universal number  $\epsilon'$  and the set  $\mathcal{N}$  of  $N_x$ s where accidental degeneracies appear. A robustness of  $\epsilon'$  and the set  $\mathcal{N}$ , both non-universal, under all three of the above deformations certainly goes beyond the low energy description of a chiral TFT in the bulk and a chiral CFT on the boundary. We also adopt this assumption in the fermionic spontaneously-chiral setting of Result 2F.

A stoquastic variant of the above assumption may also be adopted to establish the bosonic spontaneously-chiral Result 2, but a stronger statement can in fact be made, by again making use of the Frobenius-Perron theorem to resolve the accidentally degenerate ground states. The Frobenius-Perron theorem does not immediately complete the derivation of Result 2, since the former is a ground state statement, while the latter made use of the finite temperature  $\Delta E \ll \beta^{-1} \ll N_x^{-1}$ , where  $\Delta E$  is the exponentially small finite-size splitting between low lying symmetry breaking eigenstates. This difficulty does not arise in

the ‘classical symmetry breaking’ scenario, where  $\Delta E = 0$ . In the generic case  $\Delta E \neq 0$ , we can make progress under the assumption that the  $\mathcal{T}, \mathcal{P}$ -even state  $W[|+\rangle + |-\rangle]$  has lower energy than the  $\mathcal{T}, \mathcal{P}$ -odd state  $W[|+\rangle - |-\rangle]$ , rather than the opposite possibility. The derivation of Result 2 in Sec. IV A can then be repeated at zero temperature. In particular, Eq.(10) and its analysis are unchanged.

### Appendix E: A ‘non-local design principle’ for chiral topological matter

As stated in Sec. V C, the composition  $\mathbf{T} = \mathcal{P}^{(0)}\mathcal{T}^{(1/2)}$  of the spin-less reflection with the spin-1/2 time-reversal, naturally provides a design-principle for a class of models for chiral topological matter. Here we describe such  $\mathbf{T}$ -invariant models for chiral topological superconductors.

The simplest model is comprised of two copies, labeled by  $\sigma = \uparrow, \downarrow$ , of a spin-less  $p + ip$  superconductor,

$$H = \sum_{\mathbf{x}, \mathbf{x}', \sigma, \sigma'} \left[ \psi_{\sigma, \mathbf{x}}^\dagger h_{\mathbf{x}, \mathbf{x}', \sigma, \sigma'} \psi_{\sigma, \mathbf{x}'} + \psi_{\sigma, \mathbf{x}}^\dagger \Delta_{\mathbf{x} \mathbf{x}', \sigma, \sigma'} \psi_{\sigma, \mathbf{x}'}^\dagger + h.c. \right]. \quad (\text{E1})$$

Here

$$\Delta = \begin{pmatrix} \Delta_0 (d^x + id^y) & 0 \\ 0 & \Delta_0 (d^x + id^y) \end{pmatrix}, \quad (\text{E2})$$

where  $d_{\mathbf{x} \mathbf{x}'}^x$  ( $d_{\mathbf{x} \mathbf{x}'}^y$ ) is the anti-symmetric  $x$  ( $y$ ) difference operator,

$$\begin{aligned} d_{\mathbf{x} \mathbf{x}'}^x &= (\delta_{x, x'+1} - \delta_{x+1, x'}) \delta_{y, y'} / 2, \\ d_{\mathbf{x} \mathbf{x}'}^y &= \delta_{x, x'} (\delta_{y, y'+1} - \delta_{y+1, y'}) / 2, \end{aligned} \quad (\text{E3})$$

and  $\Delta_0 \in \mathbb{R} - \{0\}$ . Additionally,

$$h = \begin{pmatrix} t & 0 \\ 0 & t \end{pmatrix}, \quad (\text{E4})$$

and the hopping  $t$  is real and reflection symmetric, e.g

$$t_{\mathbf{x}, \mathbf{x}'} = \frac{1}{2} t_0 (\delta_{x, x'+1} + \delta_{x+1, x'}) \delta_{y, y'} + (x \leftrightarrow y) - \mu, \quad (\text{E5})$$

with  $t_0 > 0$ ,  $\mu \in \mathbb{R}$ . It is well known that the chemical potential  $\mu$  can be used to tune the model between gapped SPT phases with  $c = 0, -1, 1$ , for  $|\mu| > 2t_0, -2t_0 < \mu < 0, 0 < \mu < 2t_0$ , respectively, see e.g [92]. Additionally, the Hamiltonian is invariant under the combination of the unitary spin-less reflection  $\mathcal{P}^{(0)} : \psi_{\sigma, (x, y)} \mapsto \psi_{\sigma, (x, -y)}$  and the anti-unitary spin-full time-reversal  $\mathcal{T}^{(1/2)} : \psi_{\uparrow, \mathbf{x}} \mapsto \psi_{\downarrow, \mathbf{x}}, \psi_{\downarrow, \mathbf{x}} \mapsto -\psi_{\uparrow, \mathbf{x}}$ .

The model can be written in the BdG form

$$H = \sum_{\mathbf{x}, \mathbf{x}'} \Psi_{\mathbf{x}}^\dagger h_{\text{BdG}}^{\mathbf{x}, \mathbf{x}'} \Psi_{\mathbf{x}'}, \quad (\text{E6})$$

where  $\Psi_{\mathbf{x}}^T = (\psi_{\uparrow, \mathbf{x}}, \psi_{\downarrow, \mathbf{x}}, \psi_{\uparrow, \mathbf{x}}^\dagger, \psi_{\downarrow, \mathbf{x}}^\dagger)$  is the Nambu spinor (a Majorana spinor), and

$$h_{\text{BdG}} = \begin{pmatrix} h & \Delta \\ -\Delta^* & -h^* \end{pmatrix}. \quad (\text{E7})$$

The ‘single-fermion’ space on which  $h_{\text{BdG}}$  acts is  $\mathcal{H}_{1\text{F}} = \mathcal{H}_X \otimes \mathcal{H}_{\text{spin}} \otimes \mathcal{H}_{\text{Nambu}} \cong \mathbb{C}^{|X|} \otimes \mathbb{C}^2 \otimes \mathbb{C}^2$ . The spin-less reflection acts on  $\mathcal{H}_{1\text{F}}$  as  $\mathcal{P}^{(0)} = \mathcal{P}_X^{(0)} \otimes I_2 \otimes I_2$ , where  $\mathcal{P}_X^{(0)} = \delta_{x, x'} \delta_{y, -y'}$ . The spin-full time-reversal acts by  $\mathcal{T}^{(1/2)} = I_{|X|} \otimes iY \otimes I_2 \mathcal{K}$ , where  $Y$  is the Pauli matrix and  $\mathcal{K}$  is the complex conjugation. The operator  $\mathbf{T} = \mathcal{P}^{(0)}\mathcal{T}^{(1/2)}$  satisfies  $\mathbf{T}^2 = -I$  and  $[\mathbf{T}, h_{\text{BdG}}] = 0$ , and is therefore a time-reversal design principle which applies to  $h_{\text{BdG}}$ , implying  $\det(\partial_\tau + h_{\text{BdG}}) \geq 0$ . Since  $h_{\text{BdG}}$  acts on the Majorana spinor  $\Psi$ , the relevant quantity is actually the Pfaffian  $\text{Pf}(\partial_\tau + h_{\text{BdG}}) = \sqrt{\det(\partial_\tau + h_{\text{BdG}})} \geq 0$ , where the principle branch of the square root is chosen.

The Hamiltonian  $h_{\text{BdG}}$  can be considerably generalized while maintaining  $[\mathbf{T}, h_{\text{BdG}}] = 0$ , by taking

$$\begin{aligned} h &= \begin{pmatrix} t & r \\ -r^* & t^* \end{pmatrix}, \\ \Delta &= \begin{pmatrix} e^{i\alpha} (|\Delta_x| d^x + i |\Delta_y| d^y)^{|\ell|} & e^{i\tilde{\alpha}} (|\tilde{\Delta}_x| d^x + i |\tilde{\Delta}_y| d^y)^{|\tilde{\ell}|} \\ -e^{-i\tilde{\alpha}} (|\tilde{\Delta}_x| d^x + i |\tilde{\Delta}_y| d^y)^{|\tilde{\ell}|} & e^{-i\alpha} (|\Delta_x| d^x + i |\Delta_y| d^y)^{|\ell|} \end{pmatrix}, \end{aligned} \quad (\text{E8})$$

where  $t_{\mathbf{x}, \mathbf{x}'}, r_{\mathbf{x}, \mathbf{x}'}$  are general matrices, and  $\ell \in 2\mathbb{Z} + 1$  ( $\tilde{\ell} \in 2\mathbb{Z}$ ) is the angular momentum channel of the triplet (singlet) pairing. This can be further generalized to a sum over all angular momentum channels

$\sum_{\ell \in 2\mathbb{Z}+1} e^{i\alpha_\ell} (|\Delta_{\ell, x}| d^x + i |\Delta_{\ell, y}| d^y)^{|\ell|}$  and similarly for  $\tilde{\ell}$ . The model is Hermitian for  $t = t^\dagger, r = -r^T$ , but this is not required to avoid the sign problem.

In order to obtain an interacting model, the parameters

$\phi = \{t, r, \alpha_\ell, \tilde{\alpha}_{\tilde{\ell}}, |\Delta_{\ell,x}|, |\Delta_{\ell,y}|, |\tilde{\Delta}_{\tilde{\ell},x}|, |\tilde{\Delta}_{\tilde{\ell},y}|\}$  can now be promoted to space-time dependent bosonic fields, with any action  $S_\phi \in \mathbb{R}$ . The model will be sign-free as long as  $h_{\text{BdG}}$  remains  $\mathbb{T}$ -invariant for all configurations  $\phi$ , which requires that only reflection-even configurations  $\phi(\tau, x, y) = \phi(\tau, x, -y)$  are summed over. As discussed in Sec. VB, this implies non-local interactions, which effectively fold the chiral system into a non-chiral system of half of space.

## Appendix F: Locality and homogeneity of known design principles

In this appendix we review all fermionic design principles known to us, clarify their common features, and describe the conditions under which they are *on-site homogeneous*, imply a *term-wise sign-free* DQMC representation, and allow a *locally sign-free* DQMC simulation, as defined in Sec. VB. The design principles are stated as algebraic conditions satisfied by the effective single-fermion Hamiltonian  $h_\phi = h_{\phi(\tau)}$  and the corresponding imaginary-time evolution  $U_\phi = \text{TO}e^{-\int_0^\beta h_{\phi(\tau)} d\tau}$ , or in terms of the operator  $D_\phi = \partial_\tau + h_\phi$ , see Sec. VA.

*Contraction semi-groups and Majorana time reversals* The time-reversal design principle covered in Sec. VC is a special case of a broad class of design principles that were recently discovered and unified [22–24]. These are stated in terms of Majorana fermions, where  $\psi$  is real and  $\bar{\psi} = \psi^T$ , in which case  $h_\phi$  is anti-symmetric and the determinants in (17) are replaced by their square roots. Reference [24] shows that if

$$J_1 h_\phi - h_\phi^* J_1 = 0, \quad (\text{F1})$$

$$i(J_2 h_\phi - h_\phi^* J_2) \geq 0, \quad (\text{F2})$$

where the matrices  $J_1, J_2$  are real and orthogonal, and obey  $J_1^T = \pm J_1$ ,  $J_2^T = -J_2$ ,  $\{J_1, J_2\} = 0$ , then  $\text{Det}(I + U_\phi) \geq 0$ . The equality (F1) corresponds to an anti-unitary symmetry  $\mathbb{T}_1 = J_1 \mathcal{K}$ ,  $\mathbb{T}_1^2 = \pm I$ , where  $\mathcal{K}$  is the complex conjugation. If the inequality (F2) is replaced by an equality, it corresponds to an additional anti-unitary symmetry,  $\mathbb{T}_2 = J_2 \mathcal{K}$ ,  $\mathbb{T}_2^2 = -I$ . The case  $\mathbb{T}_1^2 = -I$  then reduces to the standard time-reversal  $\mathbb{T}$  described in Sec. VC, while  $\mathbb{T}_1^2 = I$  corresponds to the ‘Majorana class’ of Ref. [22]. More generally, the inequality (F2) states that the left hand side is a positive semi-definite matrix, and implies that  $h_\phi$  is a generator of the contraction semi-group defined by the Hermitian metric  $\eta_2 = iJ_2$ ,  $\eta_2^2 = I$ ,  $[\mathbb{T}_1, \eta_2] = 0$ . Explicitly, Eq.(F1)-(F2) can be written as

$$[\mathbb{T}_1, h_\phi] = 0, \quad \eta_2 h_\phi + h_\phi^\dagger \eta_2 \geq 0, \quad (\text{F3})$$

and imply

$$[\mathbb{T}_1, U_\phi] = 0, \quad \eta_2 - U_\phi^\dagger \eta_2 U_\phi \geq 0. \quad (\text{F4})$$

In the language of Sec. VB, for fixed  $\mathbb{T}_1, \eta_2$ , the set  $\mathcal{C}_h$  contains all matrices  $h_\phi$  satisfying (F3). It is clear that this set is additive:  $h_1 + h_2 \in \mathcal{C}_h$  for all  $h_1, h_2 \in \mathcal{C}_h$ . The set  $\mathcal{C}_U$  contains all matrices  $U_\phi$  satisfying Eq.(F4), and is multiplicative:  $U_1 U_2 \in \mathcal{C}_U$  for all  $U_1, U_2 \in \mathcal{C}_U$ .

A sufficient condition on  $\mathbb{T}_1, \eta_2$  that guarantees that the design principle they define is on-site homogeneous is that they are of the form  $\mathbb{T}_1 = I_{|X|} \otimes \mathbf{t}_1, \eta_2 = I_{|X|} \otimes e_2$ , written in terms of the decomposition  $\mathcal{H}_{1\text{F}} \cong \mathbb{C}^{|X|} \otimes \mathbb{C}^{\text{dF}}$  of the single-fermion space. The permutation matrices  $O^{(\sigma)}$  defined in Eq.(20) then commute with  $\eta_2$  and  $\mathbb{T}_1$ . Since  $O^{(\sigma)}$  are also unitary, we have  $O^{(\sigma)} \in \mathcal{C}_U$  for all  $\sigma \in S_X$ . All examples described in Refs. [22–24] are of the on-site homogeneous form  $\mathbb{T}_1 = I_{|X|} \otimes \mathbf{t}_1, \eta_2 = I_{|X|} \otimes e_2$ .

As in our discussion of  $\mathbb{T}$  in Sec. VC, the locality of  $\mathbb{T}_1 = I_{|X|} \otimes \mathbf{t}_1$  means that it can be applied term-wise, by symmetrizing the local terms  $h_{\phi;\mathbf{x}} \mapsto \frac{1}{2}(h_{\phi;\mathbf{x}} + \mathbb{T}_1 h_{\phi;\mathbf{x}} \mathbb{T}_1^{-1})$ . A similar procedure for  $\eta_2$  is only possible if the inequality in Eq.(F3) holds as an equality (as in Ref. [22]). The contraction semi-group defined by  $\eta_2$  then reduces to an orthogonal group, and one can enforce the term-wise relations  $\eta_2 h_{\phi;\mathbf{x}} + h_{\phi;\mathbf{x}}^\dagger \eta_2 = 0$  by  $h_{\phi;\mathbf{x}} \mapsto \frac{1}{2}(h_{\phi;\mathbf{x}} - \eta_2 h_{\phi;\mathbf{x}}^\dagger \eta_2)$ .

Collecting the above, we see that if  $\mathbb{T}_1, \eta_2$  can be brought to the form  $\mathbb{T}_1 = I_{|X|} \otimes \mathbf{t}_1, \eta_2 = I_{|X|} \otimes e_2$  by the same single-fermion local unitary  $u$ , then a DQMC representation which is  $\mathbb{T}_1$ -symmetric, and respects Eq.(F3) terms-wise, leads to a locally-sign free DQMC simulation.

*Split orthogonal group* Another recently discovered design principle is defined in terms of the split orthogonal group  $O(n, n)$  [18]: if  $U_\phi \in O(n, n)$ , then the sign of  $\text{Det}(I + U_\phi)$  depends only on the connected component of  $O(n, n)$  to which  $U_\phi$  belongs. If the sign of  $e^{-S_\phi}$  is manifestly compatible with the connected component of  $U_\phi$  in  $O(n, n)$ , one has  $p(\phi) = e^{-S_\phi} \text{Det}(I + U_\phi) \geq 0$ . More explicitly, the statement  $U_\phi \in O(n, n)$  implies that  $U_\phi$  is a real matrix and  $\eta - U_\phi^T \eta U_\phi = 0$ , where  $\eta = \text{diag}(I_n, -I_n)$ . Restricting to the identity component  $O_0(n, n)$ , this amounts to the statements that  $h_\phi$  is in the Lie algebra  $\mathfrak{o}(n, n)$ : it is real and satisfies  $\eta h_\phi + h_\phi^T \eta = 0$ .

In a basis independent formulation, the data that defines the design principle is an anti-unitary  $\tilde{\mathbb{T}}$ , such that  $\tilde{\mathbb{T}}^2 = I$ , and a Hermitian metric  $\tilde{\eta}$  with canonical form  $\eta$ , such that  $[\tilde{\mathbb{T}}, \tilde{\eta}] = 0$ . The set  $\mathcal{C}_h$  is then given by matrices  $h_\phi$  satisfying

$$[\tilde{\mathbb{T}}, h_\phi] = 0, \quad \tilde{\eta} h_\phi + h_\phi^\dagger \tilde{\eta} = 0, \quad (\text{F5})$$

while  $\mathcal{C}_U$  is defined by

$$[\tilde{\mathbb{T}}, U_\phi] = 0, \quad \tilde{\eta} - U_\phi^\dagger \tilde{\eta} U_\phi = 0. \quad (\text{F6})$$

The analogy with (F3)-(F4) is now manifest, with the inequalities strengthened to equalities. Accordingly, the  $O(n, n)$  design-principle is on-site homogeneous if  $\tilde{\mathbb{T}} = I_{|X|} \otimes \tilde{\mathbf{t}}$  and  $\tilde{\eta} = I_{|X|} \otimes \tilde{e}$ . If these forms can be obtained

by conjugation of  $\tilde{T}, \tilde{\eta}$  with the same single-fermion local unitary  $u$ , then a DQMC representation which is sign-free due to  $\tilde{T}, \tilde{\eta}$ , leads to a locally-sign free DQMC simulation.

The above statements hold for  $U_\phi$  in the identity component  $O_0(n, n)$ , which is always the case when  $h_\phi \in o(n, n)$  and  $U_\phi = \text{TO}e^{-\int_0^\beta h_{\phi(\tau)} d\tau}$ . Time evolutions in the additional three connected components of  $O(n, n)$  can be obtained by operator insertions generalizing  $U_\phi = U_k \cdots U_2 U_1$  to  $U_k \cdots O_2 U_2 O_1 U_1$ , where  $O \in O(n, n)/O_0(n, n)$  [18]. These can be incorporated into the framework of Sec.V, if each  $O_k$  is supported on a disk of radius  $w$  around a site  $\mathbf{x}_k$ , i.e.  $(O_k)_{\mathbf{x}, \mathbf{y}} = \delta_{\mathbf{x}, \mathbf{y}}$  if  $|\mathbf{x} - \mathbf{x}_k| > w$  or  $|\mathbf{y} - \mathbf{x}_k| > w$ . With this generalization, all sign-free examples described in Ref.[18] amount to locally sign-free DQMC.

*Solvable fermionic and bosonic actions* Reference [21] described a design principle that nontrivially relates the

fermionic action  $S_{\psi, \phi} = \bar{\psi} D_\phi \psi$  and bosonic action  $S_\phi$ . A fermionic action was termed 'solvable' if  $D_\phi$  has the form

$$D_\phi = \begin{pmatrix} 0 & M_\phi \\ -M_\phi^\dagger & 0 \end{pmatrix}, \quad (\text{F7})$$

which clearly implies  $\text{Det}(D_\phi) = |\text{Det}(M_\phi)|^2 \geq 0$ . Here the imaginary time circle  $\mathbb{R}/\beta\mathbb{Z}$  is discretized to  $\mathbb{Z}_\beta = \mathbb{Z}/\beta\mathbb{Z}$ , and  $D_\phi$  is treated as a matrix on  $\mathbb{C}^\beta \times \mathcal{H}_{1\text{F}} = \mathbb{C}^\beta \times \mathbb{C}^{|\mathcal{X}|} \times \mathbb{C}^{d_F}$ , with indices  $(\tau, \mathbf{x}, \alpha), (\tau', \mathbf{x}', \alpha')$  for time, space, and internal degrees of freedom. For example, the Hamiltonian form  $D_\phi = \partial_\tau + h_{\phi(\tau)}$  is discretized to

$$[D_\phi]_{(\tau, \mathbf{x}, \alpha), (\tau', \mathbf{x}', \alpha')} = (\delta_{\tau, \tau'} - \delta_{\tau-1, \tau'}) \delta_{\mathbf{x}, \mathbf{x}'} \delta_{\alpha, \alpha'} + \delta_{\tau-1, \tau'} [h_{\phi(\tau)}]_{(\mathbf{x}, \alpha), (\mathbf{x}', \alpha')}. \quad (\text{F8})$$

In a basis independent language, Eq.(F7) corresponds to

$$\{\Gamma, D_\phi\} = 0, \quad D_\phi^\dagger = -D_\phi, \quad (\text{F9})$$

where  $\Gamma$  is a 'chiral symmetry',  $\Gamma^2 = I$ ,  $\Gamma = \Gamma^\dagger$ . Eq.(19) is then obtained in a basis where  $\Gamma$  is diagonal,  $\Gamma = \text{diag}(I, -I)$ . Note however that  $\Gamma$  acts on  $D_\phi$  rather than  $h_\phi$ , and that the form (F7) requires a non-canonical transformation away from the Hamiltonian form (F8). We refer to  $\Gamma$  as on-site homogeneous if it is of the form  $\Gamma = I_\beta \otimes I_{|X|} \otimes \gamma$ , and to  $D_\phi$  as local if  $D_\phi = \sum_{\tau, \mathbf{x}} D_{\phi; \tau, \mathbf{x}}$  where each term  $D_{\phi; \tau, \mathbf{x}}$  is supported on a disk of radius  $r$  around  $(\tau, \mathbf{x})$ , and depends on the values of  $\phi$  at points within this disk. The action  $D_\phi$  is 'term-wise solvable' if each  $D_{\phi; \tau, \mathbf{x}}$  satisfies (F9). Any local  $D_\phi$  obeying (F9) with  $\Gamma = I_\beta \otimes I_{|X|} \otimes \gamma$  can be made term-wise solvable by replacing  $D_{\phi; \tau, \mathbf{x}} \mapsto \frac{1}{2}(D_{\phi; \tau, \mathbf{x}} - \Gamma D_{\phi; \tau, \mathbf{x}} \Gamma)$  and then  $D_{\phi; \tau, \mathbf{x}} \mapsto \frac{1}{2}(D_{\phi; \tau, \mathbf{x}} - D_{\phi; \tau, \mathbf{x}}^\dagger)$ . The twisted fermionic boundary conditions in (22) are implemented by declaring that the index  $(\tau = 0, \mathbf{x}, \alpha)$  that appears in Eq.(F8) corresponds to  $(\tau = \beta, x + \lambda\Theta(y), y, \alpha)$  with  $\lambda \neq 0$ . Equation (F9) then holds for all  $\lambda$  if  $\Gamma = I_\beta \otimes I_{|X|} \otimes \gamma$ . Under these conditions,

solvable fermionic actions can then be incorporated into the definition of locally sign-free DQMC given in Sec.V.

All examples given in Ref.[21] have an on-site  $\Gamma$  and local  $D_\phi$ , and it follows from the above discussion that, under these conditions, solvable fermionic actions can then be incorporated into the definition of locally sign-free DQMC given in Sec.V.

A bosonic action  $S_\phi$  for a complex valued field  $\phi = |\phi| e^{i\theta}$  was termed 'solvable' in Ref.[21] if

$$S_\phi = S_{|\phi|} - \sum_{u, u'} \beta_{u, u'} |\phi_u| |\phi_{u'}| \cos(\varepsilon_u \theta_u + \varepsilon_{u'} \theta_{u'}), \quad (\text{F10})$$

where  $u = (\mathbf{x}, \tau)$ ,  $u' = (\mathbf{x}', \tau')$ , and  $\varepsilon_u, \varepsilon_{u'} \in \{\pm 1\}$ , and  $\beta_{u, u'} \geq 0$ . For such actions, it was shown that all correlators  $\int D\phi e^{-S_\phi} \phi_{u_1} \cdots \phi_{u_k}$  are non-negative, and therefore  $\phi$  can be added to the diagonal in (F7) with a positive coupling constant  $g > 0$ ,  $D_\phi = \begin{pmatrix} g\phi & M \\ -M^\dagger & g\phi \end{pmatrix}$ , without introducing signs, though  $D_\phi$  is no longer solvable. Solvable bosonic actions are easily incorporated into the framework of Sec.V, as long as they are local in the sense of Eq.(19), and in particular,  $\beta_{u, u'} = 0$  unless the points  $u$  and  $u'$  are close.

[1] Nicholas Metropolis and S. Ulam, "The monte carlo method," *Journal of the American Statistical Association* **44**, 335–341 (1949), pMID: 18139350.

[2] Matthias Troyer and Uwe-Jens Wiese, "Computational complexity and fundamental limitations to fermionic

quantum monte carlo simulations," *Phys. Rev. Lett.* **94**, 170201 (2005).

[3] F Barahona, "On the computational complexity of ising spin glass models," *Journal of Physics A: Mathematical and General* **15**, 3241–3253 (1982).



- [4] F.F. Assaad and H.G. Evertz, “World-line and determinantal quantum monte carlo methods for spins, phonons and electrons,” *Lecture Notes in Physics* , 277–356 (2008).
- [5] Zi-Xiang Li and Hong Yao, “Sign-problem-free fermionic quantum monte carlo: Developments and applications,” *Annual Review of Condensed Matter Physics* **10**, 337–356 (2019).
- [6] Milad Marvian, Daniel A. Lidar, and Itay Hen, “On the computational complexity of curing non-stoquastic hamiltonians,” *Nature Communications* **10**, 1571 (2019).
- [7] Joel Klassen, Milad Marvian, Stephen Piddock, Marios Ioannou, Itay Hen, and Barbara Terhal, “Hardness and ease of curing the sign problem for two-local qubit hamiltonians,” *arXiv preprint arXiv:1906.08800* (2019).
- [8] Sergey Bravyi, David P. Divincenzo, Roberto Oliveira, and Barbara M. Terhal, “The complexity of stoquastic local hamiltonian problems,” *Quantum Info. Comput.* **8**, 361385 (2008).
- [9] M. B. Hastings, “How quantum are non-negative wavefunctions?” *Journal of Mathematical Physics* **57**, 015210 (2016).
- [10] Dominik Hangleiter, Ingo Roth, Daniel Nagaj, and Jens Eisert, “Easing the monte carlo sign problem,” *arXiv preprint arXiv:1906.02309* (2019).
- [11] Ribhu K Kaul, Roger G Melko, and Anders W Sandvik, “Bridging lattice-scale physics and continuum field theory with quantum monte carlo simulations,” *Annu. Rev. Condens. Matter Phys.* **4**, 179–215 (2013).
- [12] D. M. Ceperley, “Path integrals in the theory of condensed helium,” *Rev. Mod. Phys.* **67**, 279–355 (1995).
- [13] Shailesh Chandrasekharan and Uwe-Jens Wiese, “Meron-cluster solution of fermion sign problems,” *Phys. Rev. Lett.* **83**, 3116–3119 (1999).
- [14] Fakher F. Assaad and Igor F. Herbut, “Pinning the order: The nature of quantum criticality in the hubbard model on honeycomb lattice,” *Phys. Rev. X* **3**, 031010 (2013).
- [15] Shailesh Chandrasekharan and Anyi Li, “Quantum critical behavior in three dimensional lattice gross-neveu models,” *Phys. Rev. D* **88**, 021701 (2013).
- [16] Snir Gazit, Fakher F. Assaad, Subir Sachdev, Ashvin Vishwanath, and Chong Wang, “Confinement transition of  $\mathbb{Z}_2$  gauge theories coupled to massless fermions: Emergent quantum chromodynamics and  $so(5)$  symmetry,” *Proceedings of the National Academy of Sciences* **115**, E6987–E6995 (2018).
- [17] Erez Berg, Samuel Lederer, Yoni Schattner, and Simon Trebst, “Monte carlo studies of quantum critical metals,” *Annual Review of Condensed Matter Physics* **10**, 63–84 (2019).
- [18] Lei Wang, Ye-Hua Liu, Mauro Iazzi, Matthias Troyer, and Gergely Harcos, “Split orthogonal group: A guiding principle for sign-problem-free fermionic simulations,” *Phys. Rev. Lett.* **115**, 250601 (2015).
- [19] R. Blankenbecler, D. J. Scalapino, and R. L. Sugar, “Monte carlo calculations of coupled boson-fermion systems. i,” *Phys. Rev. D* **24**, 2278–2286 (1981).
- [20] Raimundo R. dos Santos, “Introduction to quantum monte carlo simulations for fermionic systems,” *Brazilian Journal of Physics* **33**, 36–54 (2003).
- [21] Shailesh Chandrasekharan, “Fermion bag approach to fermion sign problems,” *The European Physical Journal A* **49**, 90 (2013).
- [22] Zi-Xiang Li, Yi-Fan Jiang, and Hong Yao, “Majorana-time-reversal symmetries: A fundamental principle for sign-problem-free quantum monte carlo simulations,” *Phys. Rev. Lett.* **117**, 267002 (2016).
- [23] Z. C. Wei, Congjun Wu, Yi Li, Shiwei Zhang, and T. Xiang, “Majorana positivity and the fermion sign problem of quantum monte carlo simulations,” *Phys. Rev. Lett.* **116**, 250601 (2016).
- [24] Zhong-Chao Wei, “Semigroup approach to the sign problem in quantum monte carlo simulations,” *arXiv preprint arXiv:1712.09412* (2017).
- [25] C. N. Varney, C.-R. Lee, Z. J. Bai, S. Chiesa, M. Jarrell, and R. T. Scalettar, “Quantum monte carlo study of the two-dimensional fermion hubbard model,” *Phys. Rev. B* **80**, 075116 (2009).
- [26] J. P. F. LeBlanc, Andrey E. Antipov, Federico Becca, Ireneusz W. Bulik, Garnet Kin-Lic Chan, Chia-Min Chung, Youjin Deng, Michel Ferrero, Thomas M. Henderson, Carlos A. Jiménez-Hoyos, E. Kozik, Xuan-Wen Liu, Andrew J. Millis, N. V. Prokof’ev, Mingpu Qin, Gustavo E. Scuseria, Hao Shi, B. V. Svistunov, Luca F. Tocchio, I. S. Tupitsyn, Steven R. White, Shiwei Zhang, Bo-Xiao Zheng, Zhenyue Zhu, and Emanuel Gull (Simons Collaboration on the Many-Electron Problem), “Solutions of the two-dimensional hubbard model: Benchmarks and results from a wide range of numerical algorithms,” *Phys. Rev. X* **5**, 041041 (2015).
- [27] A. Kantian, M. Dolfi, M. Troyer, and T. Giamarchi, “Understanding repulsively mediated superconductivity of correlated electrons via massively parallel density matrix renormalization group,” *Phys. Rev. B* **100**, 075138 (2019).
- [28] S. Hands, I. Montvay, S. Morrison, M. Oevers, L. Scorzato, and J. Skullerud, “Numerical study of dense adjoint matter in two color qcd,” *The European Physical Journal C* **17**, 285–302 (2000).
- [29] C. R. Allton, S. Ejiri, S. J. Hands, O. Kaczmarek, F. Karsch, E. Laermann, Ch. Schmidt, and L. Scorzato, “Qcd thermal phase transition in the presence of a small chemical potential,” *Phys. Rev. D* **66**, 074507 (2002).
- [30] V. A. Goy, V. Bornyakov, D. Boyda, A. Molochkov, A. Nakamura, A. Nikolaev, and V. Zakharov, “Sign problem in finite density lattice QCD,” *Progress of Theoretical and Experimental Physics* **2017** (2017).
- [31] Mitali Banerjee, Moty Heiblum, Vladimir Umansky, Dima E Feldman, Yuval Oreg, and Ady Stern, “Observation of half-integer thermal hall conductance,” *Nature* , 1 (2018).
- [32] Chong Wang, Ashvin Vishwanath, and Bertrand I. Halperin, “Topological order from disorder and the quantized hall thermal metal: Possible applications to the  $\nu = 5/2$  state,” *Phys. Rev. B* **98**, 045112 (2018).
- [33] David F. Mross, Yuval Oreg, Ady Stern, Gilad Margalit, and Moty Heiblum, “Theory of disorder-induced half-integer thermal hall conductance,” *Phys. Rev. Lett.* **121**, 026801 (2018).
- [34] Steven H. Simon, “Interpretation of thermal conductance of the  $\nu = 5/2$  edge,” *Phys. Rev. B* **97**, 121406 (2018); D. E. Feldman, “Comment on “interpretation of thermal conductance of the  $\nu = 5/2$  edge”,” *Phys. Rev. B* **98**, 167401 (2018).
- [35] Ken K. W. Ma and D. E. Feldman, “Partial equilibration of integer and fractional edge channels in the thermal

- quantum hall effect,” *Phys. Rev. B* **99**, 085309 (2019).
- [36] Liangdong Hu, Zhao Liu, DN Sheng, FDM Haldane, and W Zhu, “Microscopic diagnosis of universal geometric responses in fractional quantum hall liquids,” arXiv preprint arXiv:2002.05565 (2020).
- [37] Michael A. Levin and Xiao-Gang Wen, “String-net condensation: A physical mechanism for topological phases,” *Phys. Rev. B* **71**, 045110 (2005).
- [38] Adam Smith, Omri Golan, and Zohar Ringel, “Intrinsic sign problems in topological quantum field theories,” arXiv preprint arXiv:2005.05343 (2020).
- [39] Zohar Ringel and Dmitry L Kovrizhin, “Quantized gravitational responses, the sign problem, and quantum complexity,” *Science advances* **3**, e1701758 (2017).
- [40] Hong-Hao Tu, Yi Zhang, and Xiao-Liang Qi, “Momentum polarization: An entanglement measure of topological spin and chiral central charge,” *Phys. Rev. B* **88**, 195412 (2013).
- [41] Michael P. Zaletel, Roger S. K. Mong, and Frank Pollmann, “Topological characterization of fractional quantum hall ground states from microscopic hamiltonians,” *Phys. Rev. Lett.* **110**, 236801 (2013).
- [42] YeJe Park and F. D. M. Haldane, “Guiding-center hall viscosity and intrinsic dipole moment along edges of incompressible fractional quantum hall fluids,” *Phys. Rev. B* **90**, 045123 (2014).
- [43] Thorsten B. Wahl, Stefan T. Haßler, Hong-Hao Tu, J. Ignacio Cirac, and Norbert Schuch, “Symmetries and boundary theories for chiral projected entangled pair states,” *Phys. Rev. B* **90**, 115133 (2014).
- [44] Thomas I. Tügel and Taylor L. Hughes, “Hall viscosity and momentum transport in lattice and continuum models of the integer quantum hall effect in strong magnetic fields,” *Phys. Rev. B* **92**, 165127 (2015).
- [45] J. Fröhlich and F. Gabbiani, “Braid statistics in local quantum theory,” *Reviews in Mathematical Physics* **02**, 251–353 (1990).
- [46] Alexei Kitaev, “Anyons in an exactly solved model and beyond,” *Annals of Physics* **321**, 2–111 (2006).
- [47] Daniel S Freed and Michael J Hopkins, “Reflection positivity and invertible topological phases,” arXiv preprint arXiv:1604.06527 (2016).
- [48] Michael H. Freedman, Michael Larsen, and Zhenghan Wang, “A modular functor which is universal for quantum computation,” *Communications in Mathematical Physics* **227**, 605–622 (2002).
- [49] Chetan Nayak, Steven H Simon, Ady Stern, Michael Freedman, and Sankar Das Sarma, “Non-abelian anyons and topological quantum computation,” *Reviews of Modern Physics* **80**, 1083 (2008).
- [50] Frank Arute, Kunal Arya, Ryan Babbush, Dave Bacon, Joseph C. Bardin, Rami Barends, Rupak Biswas, Sergio Boixo, Fernando G. S. L. Brandao, David A. Buell, Brian Burkett, Yu Chen, Zijun Chen, Ben Chiaro, Roberto Collins, William Courtney, Andrew Dunsworth, Edward Farhi, Brooks Foxen, Austin Fowler, Craig Gidney, Marissa Giustina, Rob Graff, Keith Guerín, Steve Habegger, Matthew P. Harrigan, Michael J. Hartmann, Alan Ho, Markus Hoffmann, Trent Huang, Travis S. Humble, Sergei V. Isakov, Evan Jeffrey, Zhang Jiang, Dvir Kafri, Kostyantyn Kechedzhi, Julian Kelly, Paul V. Klimov, Sergey Knysh, Alexander Korotkov, Fedor Kostritsa, David Landhuis, Mike Lindmark, Erik Lucero, Dmitry Lyakh, Salvatore Mandrà, Jarrod R. McClean, Matthew McEwen, Anthony Megrant, Xiao Mi, Kristel Michielsen, Masoud Mohseni, Josh Mutus, Ofer Naaman, Matthew Neeley, Charles Neill, Murphy Yuezhen Niu, Eric Ostby, Andre Petukhov, John C. Platt, Chris Quintana, Eleanor G. Rieffel, Pedram Roushan, Nicholas C. Rubin, Daniel Sank, Kevin J. Satzinger, Vadim Smelyanskiy, Kevin J. Sung, Matthew D. Trevithick, Amit Vainsencher, Benjamin Villalonga, Theodore White, Z. Jamie Yao, Ping Yeh, Adam Zalcman, Hartmut Neven, and John M. Martinis, “Quantum supremacy using a programmable superconducting processor,” *Nature* **574**, 505–510 (2019).
- [51] CL Kane and Matthew PA Fisher, “Quantized thermal transport in the fractional quantum hall effect,” *Physical Review B* **55**, 15832 (1997).
- [52] Nicholas Read and Dmitry Green, “Paired states of fermions in two dimensions with breaking of parity and time-reversal symmetries and the fractional quantum hall effect,” *Physical Review B* **61**, 10267 (2000).
- [53] Andrea Cappelli, Marina Huerta, and Guillermo R Zemba, “Thermal transport in chiral conformal theories and hierarchical quantum hall states,” *Nuclear Physics B* **636**, 568–582 (2002).
- [54] Anton Kapustin and Lev Spodyneiko, “Thermal hall conductance and a relative topological invariant of gapped two-dimensional systems,” arXiv preprint arXiv:1905.06488 (2019).
- [55] Sébastien Jezouin, FD Parmentier, A Anthore, U Gennser, A Cavanna, Y Jin, and F Pierre, “Quantum limit of heat flow across a single electronic channel,” *Science* **342**, 601–604 (2013).
- [56] Mitali Banerjee, Moty Heiblum, Amir Rosenblatt, Yuval Oreg, Dima E Feldman, Ady Stern, and Vladimir Umansky, “Observed quantization of anyonic heat flow,” *Nature* **545**, 75 (2017).
- [57] Y. Kasahara, T. Ohnishi, Y. Mizukami, O. Tanaka, Sixiao Ma, K. Sugii, N. Kurita, H. Tanaka, J. Nasu, Y. Motome, T. Shibauchi, and Y. Matsuda, “Majorana quantization and half-integer thermal quantum hall effect in a kitaev spin liquid,” *Nature* **559**, 227–231 (2018).
- [58] Alexander G Abanov and Andrey Gromov, “Electromagnetic and gravitational responses of two-dimensional non-interacting electrons in a background magnetic field,” *Physical Review B* **90**, 014435 (2014).
- [59] Semyon Klevtsov and Paul Wiegmann, “Geometric adiabatic transport in quantum hall states,” *Physical review letters* **115**, 086801 (2015).
- [60] Barry Bradlyn and N Read, “Topological central charge from berry curvature: Gravitational anomalies in trial wave functions for topological phases,” *Physical Review B* **91**, 165306 (2015).
- [61] Omri Golan, Carlos Hoyos, and Sergej Moroz, “Boundary central charge from bulk odd viscosity: Chiral superfluids,” *Phys. Rev. B* **100**, 104512 (2019).
- [62] T Can, YH Chiu, M Laskin, and P Wiegmann, “Emergent conformal symmetry and geometric transport properties of quantum hall states on singular surfaces,” *Physical review letters* **117**, 266803 (2016).
- [63] Nathan Schine, Albert Ryou, Andrey Gromov, Ariel Sommer, and Jonathan Simon, “Synthetic landau levels for photons,” *Nature* **534**, 671 (2016).

- [64] Nathan Schine, Michelle Chalupnik, Tankut Can, Andrey Gromov, and Jonathan Simon, “Measuring electromagnetic and gravitational responses of photonic landau levels,” arXiv preprint arXiv:1802.04418 (2018).
- [65] Rajarshi Bhattacharyya, Mitali Banerjee, Moty Heiblum, Diana Mahalu, and Vladimir Umansky, “Melting of interference in the fractional quantum hall effect: Appearance of neutral modes,” *Phys. Rev. Lett.* **122**, 246801 (2019).
- [66] Bernd Rosenow, Ivan P. Levkivskyi, and Bertrand I. Halperin, “Current correlations from a mesoscopic anyon collider,” *Phys. Rev. Lett.* **116**, 156802 (2016).
- [67] H. Bartolomei, M. Kumar, R. Bisognin, A. Marguerite, J.-M. Berroir, E. Bocquillon, B. Plaçais, A. Cavanna, Q. Dong, U. Gennser, Y. Jin, and G. Fève, “Fractional statistics in anyon collisions,” *Science* **368**, 173–177 (2020).
- [68] Parsa Hassan Bonderson, *Non-Abelian anyons and interferometry*, Ph.D. thesis, California Institute of Technology (2007).
- [69] Tian Lan, Liang Kong, and Xiao-Gang Wen, “Theory of (2+1)-dimensional fermionic topological orders and fermionic/bosonic topological orders with symmetries,” *Phys. Rev. B* **94**, 155113 (2016).
- [70] Po-Shen Hsin, Ying-Hsuan Lin, Natalie M. Paquette, and Juven Wang, “An effective field theory for fractional quantum hall systems near  $\nu = 5/2$ ,” arXiv preprint arXiv:2005.10826 (2020).
- [71] Juven Wang, Xiao-Gang Wen, and Edward Witten, “Symmetric gapped interfaces of spt and set states: Systematic constructions,” *Phys. Rev. X* **8**, 031048 (2018).
- [72] Bei Zeng, Xie Chen, Duan-Lu Zhou, and Xiao-Gang Wen, *Quantum information meets quantum matter* (Springer, 2019).
- [73] Xie Chen, Zheng-Cheng Gu, Zheng-Xin Liu, and Xiao-Gang Wen, “Symmetry protected topological orders and the group cohomology of their symmetry group,” arXiv preprint arXiv:1106.4772 (2011).
- [74] Anton Kapustin, Ryan Thorngren, Alex Turzillo, and Zitao Wang, “Fermionic symmetry protected topological phases and cobordisms,” *Journal of High Energy Physics* **2015**, 1–21 (2015).
- [75] Anton Kapustin and Ryan Thorngren, “Fermionic spt phases in higher dimensions and bosonization,” *Journal of High Energy Physics* **2017** (2017), 10.1007/jhep10(2017)080.
- [76] Xiao-Liang Qi and Shou-Cheng Zhang, “Topological insulators and superconductors,” *Reviews of Modern Physics* **83**, 1057 (2011).
- [77] X. G. WEN, “Topological orders in rigid states,” *International Journal of Modern Physics B* **04**, 239–271 (1990), <https://doi.org/10.1142/S0217979290000139>.
- [78] Xie Chen, Zheng-Cheng Gu, and Xiao-Gang Wen, “Local unitary transformation, long-range quantum entanglement, wave function renormalization, and topological order,” *Phys. Rev. B* **82**, 155138 (2010).
- [79] L. Cincio and G. Vidal, “Characterizing topological order by studying the ground states on an infinite cylinder,” *Phys. Rev. Lett.* **110**, 067208 (2013).
- [80] Lucile Savary and Leon Balents, “Quantum spin liquids: a review,” *Reports on Progress in Physics* **80**, 016502 (2016).
- [81] Michael Levin and Ady Stern, “Fractional topological insulators,” *Phys. Rev. Lett.* **103**, 196803 (2009).
- [82] Ady Stern, “Fractional topological insulators: A pedagogical review,” *Annual Review of Condensed Matter Physics* **7**, 349–368 (2016), <https://doi.org/10.1146/annurev-conmatphys-031115-011559>.
- [83] Paul Ginsparg, “Applied conformal field theory,” arXiv preprint hep-th/9108028 (1988).
- [84] P. Di Francesco, P. Mathieu, and D. Sénéchal, *Conformal Field Theory*, Graduate texts in contemporary physics (Island Press, 1996).
- [85] F. D. M. Haldane, “Model for a quantum hall effect without landau levels: Condensed-matter realization of the “parity anomaly”,,” *Phys. Rev. Lett.* **61**, 2015–2018 (1988).
- [86] Xiao-Liang Qi, Taylor L Hughes, and Shou-Cheng Zhang, “Topological field theory of time-reversal invariant insulators,” *Physical Review B* **78**, 195424 (2008).
- [87] Shinsei Ryu, Andreas P Schnyder, Akira Furusaki, and Andreas WW Ludwig, “Topological insulators and superconductors: tenfold way and dimensional hierarchy,” *New Journal of Physics* **12**, 065010 (2010).
- [88] Hidenori Takagi, Tomohiro Takayama, George Jackeli, Giniyat Khaliullin, and Stephen E Nagler, “Concept and realization of kitaev quantum spin liquids,” *Nature Reviews Physics* **1**, 264–280 (2019).
- [89] Edward Witten, “Quantum field theory and the jones polynomial,” *Communications in Mathematical Physics* **121**, 351–399 (1989).
- [90] Andrey Gromov, Gil Young Cho, Yizhi You, Alexander G Abanov, and Eduardo Fradkin, “Framing anomaly in the effective theory of the fractional quantum hall effect,” *Physical review letters* **114**, 016805 (2015).
- [91] Andrey Gromov, Kristan Jensen, and Alexander G Abanov, “Boundary effective action for quantum hall states,” *Physical review letters* **116**, 126802 (2016).
- [92] Omri Golan and Ady Stern, “Probing topological superconductors with emergent gravity,” *Phys. Rev. B* **98**, 064503 (2018).
- [93] Heidar Moradi and Xiao-Gang Wen, “Universal wavefunction overlap and universal topological data from generic gapped ground states,” *Phys. Rev. Lett.* **115**, 036802 (2015).
- [94] Alexander Altland and Ben D Simons, *Condensed matter field theory* (Cambridge University Press, 2010).
- [95] Jing Yu, Xing-Hai Zhang, and Su-Peng Kou, “Majorana edge states for  $F_2$  topological orders of the wen plaquette and toric code models,” *Phys. Rev. B* **87**, 184402 (2013).
- [96] Seth Lloyd, “Universal quantum simulators,” *Science* **273**, 1073–1078 (1996).
- [97] Jia-Wei Mei and Xiao-Gang Wen, “Modular matrices from universal wave-function overlaps in gutzwiller-projected parton wave functions,” *Phys. Rev. B* **91**, 125123 (2015).
- [98] GE Volovik, *The universe in a helium droplet* (Oxford University Press New York, 2009).
- [99] Félix Rose, Omri Golan, and Sergej Moroz, “Hall viscosity and conductivity of two-dimensional chiral superconductors,” arXiv preprint arXiv:2004.02590 (2020).
- [100] Subir Sachdev, *Quantum Phase Transitions*, 2nd ed. (Cambridge University Press, 2011).
- [101] S. M. A. Rombouts, K. Heyde, and N. Jachowicz, “Quantum monte carlo method for fermions, free of discretization errors,” *Phys. Rev. Lett.* **82**, 4155–4159 (1999).
- [102] Congjun Wu and Shou-Cheng Zhang, “Sufficient condition

- for absence of the sign problem in the fermionic quantum monte carlo algorithm,” *Phys. Rev. B* **71**, 155115 (2005).
- [103] Johannes S Hofmann, Fakhre F Assaad, Raquel Queiroz, and Eslam Khalaf, “A search for correlation-induced adiabatic paths between distinct topological insulators,” *arXiv preprint arXiv:1912.07614* (2019).
  - [104] Joji Nasu, Junki Yoshitake, and Yukitoshi Motome, “Thermal transport in the kitaev model,” *Phys. Rev. Lett.* **119**, 127204 (2017).
  - [105] Zheng-Cheng Gu, Zhenghan Wang, and Xiao-Gang Wen, “Classification of two-dimensional fermionic and bosonic topological orders,” *Phys. Rev. B* **91**, 125149 (2015).
  - [106] Mikio Nakahara, *Geometry, topology and physics* (CRC Press, 2003).
  - [107] Yi Zhang, Tarun Grover, Ari Turner, Masaki Oshikawa, and Ashvin Vishwanath, “Quasiparticle statistics and braiding from ground-state entanglement,” *Phys. Rev. B* **85**, 235151 (2012).
  - [108] Heidar Moradi and Xiao-Gang Wen, “Universal topological data for gapped quantum liquids in three dimensions and fusion algebra for non-abelian string excitations,” *Phys. Rev. B* **91**, 075114 (2015).
  - [109] Huan He, Heidar Moradi, and Xiao-Gang Wen, “Modular matrices as topological order parameter by a gauge-symmetry-preserved tensor renormalization approach,” *Phys. Rev. B* **90**, 205114 (2014).
  - [110] Jia-Wei Mei, Ji-Yao Chen, Huan He, and Xiao-Gang Wen, “Gapped spin liquid with  $F_2$  topological order for the kagome heisenberg model,” *Phys. Rev. B* **95**, 235107 (2017).
  - [111] Qi Zhang, Zi-Qi Wang, and Guang-Ming Zhang, “Non-hermitian effects of the intrinsic signs in topologically ordered wavefunctions,” *arXiv preprint arXiv:2005.03841* (2020).
  - [112] Tianxing Ma, Zhongbing Huang, Feiming Hu, and Hai-Qing Lin, “Pairing in graphene: A quantum monte carlo study,” *Phys. Rev. B* **84**, 121410 (2011).
  - [113] Annica M Black-Schaffer and Carsten Honerkamp, “Chiral-d-wave superconductivity in doped graphene,” *Journal of Physics: Condensed Matter* **26**, 423201 (2014).
  - [114] Chien-Hung Lin and Michael Levin, “Generalizations and limitations of string-net models,” *Phys. Rev. B* **89**, 195130 (2014).
  - [115] Andrew C Potter and Ashvin Vishwanath, “Protection of topological order by symmetry and many-body localization,” *arXiv preprint arXiv:1506.00592* (2015).
  - [116] Nathanan Tantivasadakarn and Ashvin Vishwanath, “Full commuting projector hamiltonians of interacting symmetry-protected topological phases of fermions,” *Phys. Rev. B* **98**, 165104 (2018).
  - [117] T. B. Wahl, H.-H. Tu, N. Schuch, and J. I. Cirac, “Projected entangled-pair states can describe chiral topological states,” *Phys. Rev. Lett.* **111**, 236805 (2013).
  - [118] J. Dubail and N. Read, “Tensor network trial states for chiral topological phases in two dimensions and a no-go theorem in any dimension,” *Phys. Rev. B* **92**, 205307 (2015).
  - [119] Ji-Yao Chen, Laurens Vanderstraeten, Sylvain Capponi, and Didier Poilblanc, “Non-abelian chiral spin liquid in a quantum antiferromagnet revealed by an ipeps study,” *Phys. Rev. B* **98**, 184409 (2018).
  - [120] Jun Ho Son and Jason Alicea, “Commuting-projector hamiltonians for chiral topological phases built from parafermions,” *Phys. Rev. B* **97**, 245144 (2018).
  - [121] Giacomo Torlai, Juan Carrasquilla, Matthew T. Fishman, Roger G. Melko, and Matthew P. A. Fisher, “Wavefunction positization via automatic differentiation,” *arXiv preprint arXiv:1906.04654* (2019).
  - [122] Michael P. Zaletel, “Detecting two-dimensional symmetry-protected topological order in a ground-state wave function,” *Phys. Rev. B* **90**, 235113 (2014).
  - [123] Anton Kapustin, Ryan Thorngren, Alex Turzillo, and Zitao Wang, “Fermionic symmetry protected topological phases and cobordisms,” *Journal of High Energy Physics* **2015**, 1–21 (2015).
  - [124] Edward Witten, “Fermion path integrals and topological phases,” *Rev. Mod. Phys.* **88**, 035001 (2016).
  - [125] Ken Shiozaki, Hassan Shapourian, and Shinsei Ryu, “Many-body topological invariants in fermionic symmetry-protected topological phases: Cases of point group symmetries,” *Phys. Rev. B* **95**, 205139 (2017).
  - [126] Ken Shiozaki, Hassan Shapourian, Kiyonori Gomi, and Shinsei Ryu, “Many-body topological invariants for fermionic short-range entangled topological phases protected by antiunitary symmetries,” *Phys. Rev. B* **98**, 035151 (2018).
  - [127] R. Bondesan and Z. Ringel, “Classical topological paramagnetism,” *Phys. Rev. B* **95**, 174418 (2017).
  - [128] Scott D. Geraedts and Olexei I. Motrunich, “Monte carlo study of a  $u(1) \times u(1)$  system with  $\pi$ -statistical interaction,” *Phys. Rev. B* **85**, 045114 (2012).
  - [129] Scott D. Geraedts and Olexei I. Motrunich, “Phases and phase transitions in a  $u(1) \times u(1)$  system with  $\theta = 2\pi/3$  mutual statistics,” *Phys. Rev. B* **86**, 045106 (2012).
  - [130] Snir Gazit and Ashvin Vishwanath, “Bosonic topological phase in a paired superfluid,” *Phys. Rev. B* **93**, 115146 (2016).
  - [131] Tian Lan, Liang Kong, and Xiao-Gang Wen, “Classification of (2+1)-dimensional topological order and symmetry-protected topological order for bosonic and fermionic systems with on-site symmetries,” *Phys. Rev. B* **95**, 235140 (2017).
  - [132] David Aasen, Ethan Lake, and Kevin Walker, “Fermion condensation and super pivotal categories,” *Journal of Mathematical Physics* **60**, 121901 (2019).
  - [133] A.Yu. Kitaev, “Fault-tolerant quantum computation by anyons,” *Annals of Physics* **303**, 2 – 30 (2003).
  - [134] M. Fremling, T. H. Hansson, and J. Suorsa, “Hall viscosity of hierarchical quantum hall states,” *Phys. Rev. B* **89**, 125303 (2014).